



Interest of Bone Histomorphometry in Bone Pathophysiology Investigation: Foundation, Present, and Future

Pascale Chavassieux* and Roland Chapurlat

Université de Lyon, INSERM, UMR 1033, Lyon, France

Despite the development of non-invasive methods, bone histomorphometry remains the only method to analyze bone at the tissue and cell levels. Quantitative analysis of transiliac bone sections requires strict methodologic conditions but since its foundation more 60 years ago, this methodology has progressed. Our purpose was to review the evolution of bone histomorphometry over the years and its contribution to the knowledge of bone tissue metabolism under normal and pathological conditions and the understanding of the action mechanisms of therapeutic drugs in humans. The two main applications of bone histomorphometry are the diagnosis of bone diseases and research. It is warranted for the diagnosis of mineralization defects as in osteomalacia, of other causes of osteoporosis as bone mastocytosis, or the classification of renal osteodystrophy. Bone biopsies are required in clinical trials to evaluate the safety and mechanism of action of new therapeutic agents and were applied to anti-osteoporotic agents such as bisphosphonates and denosumab, an anti-RANKL, which induces a marked reduction of the bone turnover with a consequent elongation of the mineralization period. In contrast, an increased bone turnover with an extension of the formation site is observed with teriparatide. Romosozumab, an anti-sclerostin, has a dual effect with an early increased formation and reduced resorption. Bone histomorphometric studies allow us to understand the mechanism of coupling between formation and resorption and to evaluate the respective role of bone modeling and remodeling. The adaptation of new image analysis techniques will help bone biopsy analysis in the future.

Keywords: bone biopsy, histomorphometry, bone disease, modeling, remodeling, mechanism of action of treatment

OPEN ACCESS

Edited by:

Daniela Merlotti,
University of Siena, Italy

Reviewed by:

Toshio Matsumoto,
Tokushima University, Japan
Luca Dalle Carbonare,
University of Verona, Italy

*Correspondence:

Pascale Chavassieux
pascale.chavassieux@univ-lyon1.fr

Specialty section:

This article was submitted to
Bone Research,
a section of the journal
Frontiers in Endocrinology

Received: 30 March 2022

Accepted: 22 June 2022

Published: 28 July 2022

Citation:

Chavassieux P and Chapurlat R (2022)
Interest of Bone Histomorphometry in
Bone Pathophysiology Investigation:
Foundation, Present, and Future.
Front. Endocrinol. 13:907914.
doi: 10.3389/fendo.2022.907914

INTRODUCTION

Despite the development of non-invasive methods as bone densitometry, biochemical markers, and quantitative computed tomography, bone histomorphometry remains the only method for the study of bone at the tissue and cellular levels. This method enables measurements at intermediary levels of bone organization, i.e., the osteon in cortical bone and the bone structural unit (BSU) in cancellous bone. Bone histomorphometry consists of counting the cells and measuring the bone

tissue components. The field of bone histomorphometry appeared in the early 1960s and markedly progressed over the following decades. The sequence of activation-resorption-formation and the basic multicellular unit (BMU) initially described by Frost (1–3) led to defining the concept of bone remodeling. Each remodeling site gives rise to a BSU (4) which constitutes bone tissue. In addition to the measurements of static parameters which give an imprint of previous remodeling events, the introduction of double labeling with tetracycline, which is laid down at the mineralization front, provides a time dimension (3). The methods used for the measurements on histological sections are based on Delesse's principle (5) which allows the deduction of 3D parameters from 2D measurements. A variance in the bone histomorphometric measurements may be observed which results from the methodology used and the inter-observer variation. The main methodological factors are the sampling, staining procedures, and the measuring methods. For these reasons bone histomorphometry requires strict and standardized methodological conditions. The diagnosis of the majority of bone diseases is based on clinical, radiological, and biochemical examinations but a bone biopsy can be required to evaluate a mineralization defect, to determine the form of renal osteodystrophy, or to understand a non-response to treatment. Bone histomorphometry is the only method for the analysis of the pathophysiology of bone diseases and is mandatory for the safety and mechanism of action of new drug at the tissue and cellular levels. It also allows to investigate and understand the mechanism of coupling between resorption and formation during the remodeling process and the role of the modeling. Our purpose was to review the evolution of bone histomorphometry across the years including the improvement in the methods, the development of new parameters, the conditions required for a suitable analysis, the knowledge in bone tissue metabolism under normal and pathological conditions, and the understanding of the mechanisms of action of therapeutic drugs in humans. We also considered future applications.

BONE BIOPSY

A bone biopsy is necessary to obtain a bone sample.

Procedure

A horizontal transiliac bone biopsy is the preferred method (6). It gives a sample with two cortices and a sufficient amount of spongy bone (7), in contrast to the vertical biopsy which provides only one cortex (8). Transiliac bone biopsy must be taken at the standard site i.e., 2 cm below the summit of the iliac crest and 2 cm behind the antero-superior iliac spine. It requires local anesthesia of both the internal and external periosteum. Bone biopsy is safe and generally well-tolerated. The incidence of complications reported is low, at 0.52% with mainly hematomas, pain, transient femoral neuropathy, and skin infection (9). If a follow-up biopsy must be performed, it must be done on the opposite side to avoid the prior callus. Several

types of trephines for bone biopsy have been used (7). The 2 mm diameter Jamshidi needle (10) does not allow for suitable evaluation of bone turnover and mineralization (11). Trephines with a diameter of 5 mm were responsible for a large sampling variation (12, 13). A trephine of 7.5 mm inner diameter, as Bordier trephine modified by Meunier, provides a transiliac sample with two cortices and a sufficient amount of spongy bone suitable for histomorphometry. An electrically driven trephine has also been proposed (14). The trephine teeth must be perfectly sharpened to avoid compression artifacts and fracture of the specimen which may compromise the analysis. The experience of the operator is another factor that contributes to the quality of the sample (9).

In Vivo Tetracycline Labeling

Prior to biopsy, the administration of fluorochromes allows the measurement of dynamic parameters of bone formation and consequently under specific conditions, the assessment of bone turnover. There are several fluorochrome regimens (15, 16) but tetracycline is a safe tissue marker (3). Tetracycline incorporates into new bone at the time of the mineralization and remains as long as the bone is not resorbed (17). Alizarin, another tissue marker, inhibits the bone formation and must not be used in humans (18). Its use must be limited to animal studies and given just before the biopsy. Different tetracycline regimens have been used and the choice mainly depends on the availability in the center. They are equivalent despite some differences observed with respect to their uptake by the mineralizing bone. Parfitt et al. (19) showed that the extent of surfaces labeled with demethylchlortetracycline were higher than with oxytetracycline. The difference may be explained by a lower blood level, a shorter half-life, and a lower affinity for binding to the crystal for oxytetracycline than demethylchlortetracycline (20). Different schedules of double labelings are used but the current procedure is to administer tetracycline for two sequences of 2 days 10 days apart, with the biopsy being performed 3–5 days after. Tetracycline deposited, along the calcification front in bone, appears as two distinct lines visualized on unstained bone sections under ultraviolet light (3) (**Figure 1**). More recently, another labeling schedule has been proposed (21). It is based on a quadruple labeling with a first double labeling at baseline and a second one a few months later (≤ 3 months). This method allows longitudinal analysis of short-term changes of bone formation in one single biopsy. This technique presents two advantages over paired biopsies: only one sample is collected in each patient and each serves as his/her own pre-treatment control, eliminating problems due to the inter-individual variability in histomorphometric variables (22). The second labelling must be administered less than three months after the first one to avoid the resorption of the first set of labels and to allow the calculation of parameters expressed with bone surface as referent because bone surfaces used for the calculation of the baseline parameters are those measured at the time of biopsy. The potential variation of the extent of bone surface after 1–2 months is very low and markedly lower than the inter-individual variation.

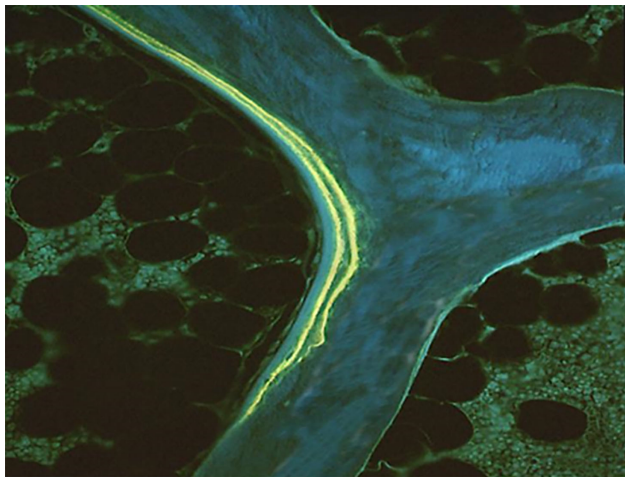


FIGURE 1 | Double tetracycline labels. Unstained section under ultraviolet light; x100.

Histological Techniques

Fixation and Embedding

Bone samples must be processed without prior decalcification. Upon the collection, the sample must be placed in fixative, methanol, 70% ethanol, or 10% phosphate-buffered formalin (pH 7). However, alcoholic fixatives are recommended to preserve the tetracycline labels. The embedding compound must be as hard as the calcified bone to preserve the integrity of the bone architecture during sectioning. Different embedding materials have been used such as Epon or Bioplastic but methyl or glycol methacrylate are the most convenient (23, 24). In addition, these plastics may be dissolved before staining but this procedure may damage the bone architecture. As polymerization of methacrylates is an exothermic reaction, enzyme activity and antigenic characters are lost by high temperatures. Several authors have reported modifications of the conventional methacrylate techniques performed at low temperatures allowing the preservation of enzymes activities (25–28)

Sectioning

Sections, 5 to 20 μm thick, are cut using special microtomes equipped with tungsten carbide-edged knives or with diamond or glass knives (24). Sections can be also obtained by polishing. These knives must be perfectly sharpened to obtain sections of good quality. The block is oriented so that the cortices are perpendicular to the knife edge. It is recommended to obtain two or three sets of sections in the central part of the sample, separated by 200–300 μm to avoid replicate sampling of a single surface event (29–31).

Staining

The initial objectives of stain were to unequivocally differentiate osteoid and mineralized bone and to identify cells. Von Kossa was initially recognized as the reference method (24, 32) but it was not

ideal for cellular details. Villanueva osteochrome and tetrachrome have also been used (33) and a modification of the osteochrome was described and allowed the simultaneous assessment of tetracycline and osteoid seams (34). Solochrome Cyanin R (35) is very good for staining osteoid and for observing the bone texture under polarized light (**Figure 2A**) but the manufacturer ceased production several years ago. A stain for osteoid tissue in the fresh, unembedded bone sample has also been reported (36). Toluidine blue stains the calcification front as a granular metachromatic dark line but the most suitable way to identify the calcification front is the use of tetracycline labeling (37). Today, Goldner's trichrome is the most widely used (38–40). It allows a clear identification of osteoid and bone cells with a sufficient contrast for analyses with image analyzers (**Figure 2B**).

Besides the assessment of bone structure and remodeling, specific staining techniques are applied for either diagnosis or research purposes. The diagnosis of a bone mastocytosis is confirmed by the count of mast cells on histological bone sections. Mast cells are identified on sections stained with May-Grünwald-Giemsa, acridine orange or toluidine blue pH 2.6. Based on the principles of metachromasia, mast cells granules are stained purple by toluidine blue pH 2.6 (41, 42) (**Figure 2C**). The contamination of dialysis with aluminum led to the accumulation in patients with chronic renal failure undergoing haemodialysis (43). Aluminum accumulation has also been reported after regular consumption of aluminum-based antacids (44). Overload of aluminum was shown to be responsible for vitamin D resistant osteomalacia. Measurement of serum aluminum was not sufficiently discriminant for assessment of aluminum intoxication in these patients. Bone aluminum can be shown by a specific histochemical staining with aurine tricarboxylic acid (aluminon staining). Aluminum deposits appear as a deep pink to red line on the mineralized surfaces (**Figure 2D**) (45–47). Other stainings have been reported such as acid solochrome azurine (Mordant blue) or a technique described by Walton et al. (48) where aluminum forms a complex with the carboxylate group of the phoxine dye.

Osteoclasts are known to have a high tartrate-resistant acid phosphatase (TRAP) content. A staining procedure allows specific identification of osteoclastic acid phosphatase. This technique has been shown to stain only osteoclastic acid phosphatase enzymes and not induce artifacts (49). As previously mentioned, it requires a prior embedding process at low temperature to not alter the enzyme activity. TRAP is located in lysosomes and reflects the osteoclasts function (50, 51) (**Figure 2E**).

Bone microdamage is essential in the assessment of bone quality because its accumulation, due to fatigue loading, may lead to fracture (52). The method allowing the detection of microdamage in bone must distinguish *in vitro* microdamage caused by the histological process from the naturally occurring one. This requires making bulk staining, i.e., staining before embedding and sectioning. The first technique used basic fuchsin (53). However basic fuchsin is not specific because it binds to exposed collagen but does not bind to the mineral phase (54). Different dyes such as oxytetracycline, xylenol orange, green

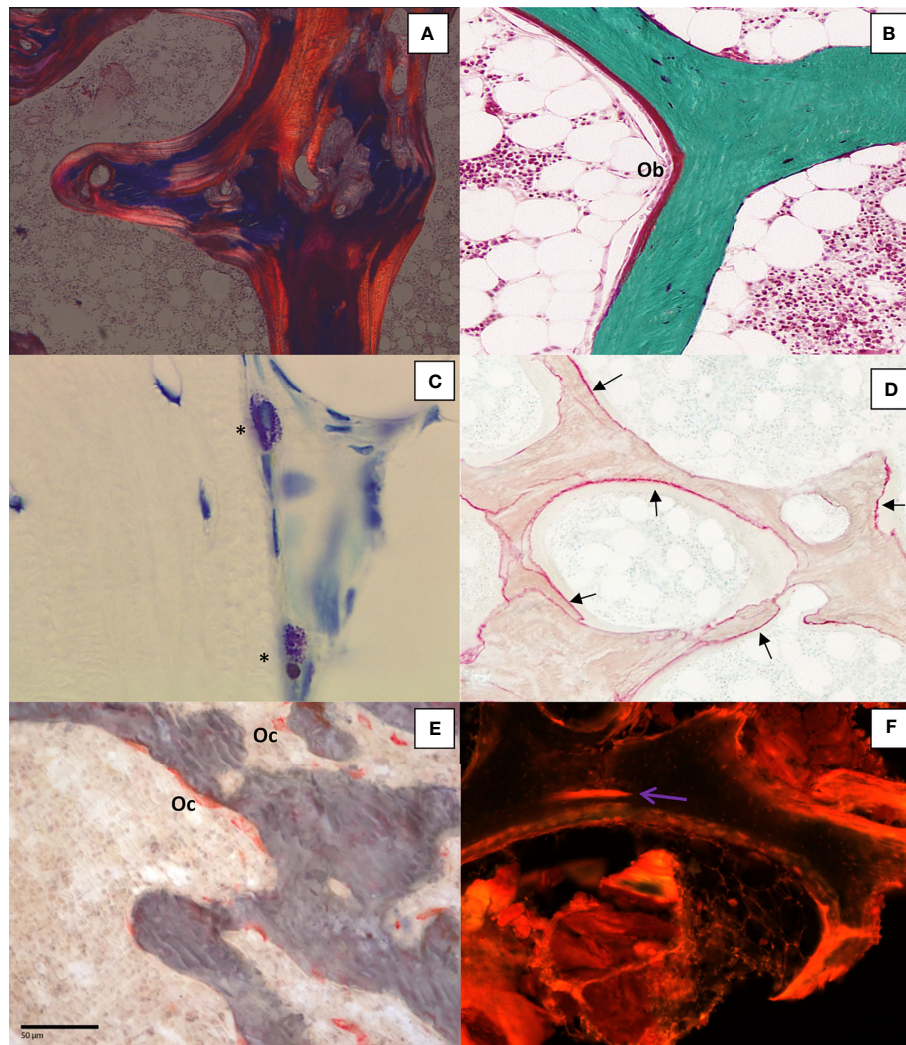


FIGURE 2 | (A) Bone section stained with solochrome cyanin R under polarized light showing the lamellar texture of bone tissue (x100); **(B)** Goldner trichrome differentiates mineralized bone in green and osteoid seam covered by osteoblasts (Ob) in red (x200); **(C)** Mast cells (*) in bone marrow characterized by the presence of metachromatic granules in the cytoplasm after toluidin blue pH 2.6 staining (x400); **(D)** Aluminon staining showing the aluminum deposition (→) along the calcification front (x100); **(E)** TRAP staining of osteoclasts (Oc) (x200); **(F)** Microcrack (→) stained after bulk staining with xylenol orange (x200).

calcein, and calcein blue bind microcracks (55). They fluoresce at different wavelengths and colors and can be sequentially used to follow the progression of microcracks *in vitro* (56). Some dye, e.g., xylenol orange, do not hamper the reading of tetracycline labeling (57) (**Figure 2F**).

Several years ago, techniques staining the cement lines were described. They were based on the use of either gallocyenin associated with Villanueva which stained cement lines in blue or purple (40) or toluidine blue dissolved in 0.1% formic acid (58) which stained cement lines in dark blue. More recently, the interest of analyzing the cement lines has been raised to identify remodeling and modeling-based formation. To date, these two phenomena were usually differentiated by the morphological aspect of these cement lines which, by definition, are crenated after remodeling and smooth after modeling. Recently, an

immunostaining of osteopontin has been reported, which differentiates osteopontin-rich smooth cement lines formed by modeling from osteopontin-poor scalloped cement lines generated by remodeling process (59).

HISTOMORPHOMETRY

Stereological Principles

Bone histomorphometry consists in the measurement of a three-dimensional structure on a two-dimensional thin section. Basic stereological theorems based on the Delesse principle (5) report the mathematical proofs that a volume can be extrapolated from the area of its profiles and there is a relationship between its surface and the profile of its boundary length (60–64). However,

the prerequisite of most stereologic theorems is that the structure is isotropic, i.e., dispersed and randomly oriented in the space (65, 66). This condition is not always fulfilled in bone, as the microarchitecture is mainly determined by the mechanical forces, except in iliac bone. In cortical bone, the main axis of the Haversian canals is parallel to the longitudinal axis of the diaphyseal cortex (67) and cancellous bone consists of trabeculae more or less oriented (68). Random, but anisotropic, sections obtained with a fix axis and called “vertical sections”, can provide an unbiased estimation (69). This sampling procedure has been applied to bone by Vesterby et al. (70) where the vertical axis is parallel to the cylindrical core surface, the sections are obtained with a random rotation around the axis, and a cycloid test grid is used.

Measuring Methods

Validation

Different methods have been used for the quantification of the bone components. The first step before using a method is its validation, i.e., the evaluation of accuracy, reproducibility, and linearity.

The accuracy depends on the lack of bias and the precision. Measurements are biased when they systematically differ from the true value. The precision is given by the narrow dispersion of measurements (66). The reproducibility reflects the variation between repeated measurements performed either by the same observer (intra-observer variability) or by different observers having the same experience (inter-observer variability). The linearity assesses the relationship between the measures and the true values for a large range of values. These evaluations are performed by using standard micrometers for image analyzers and standard bone sections and are applied for the measurements of distance, length, and area.

Methods

Initially, the measurements were performed with a manual point-counting method using integrative eyepieces which consisted of projecting straight or semicircle parallel lines and points on the microscopic field (66). More recently, this method has been almost abandoned and replaced by interactive computerized analyzers.

Semi-automatic systems are composed of a microscope equipped with a drawing tube, a digitizing tablet, and a cursor. The image of the cursor light is projected on the microscopic field and the measurement is performed by tracing the structure to be measured on the digitizing tablet. The x and y coordinates of each point of the tablet are integrated by a computer which gives the results according to the previously selected program package (71–73).

With the development of computerized technique, the automatic method image analyzer processes, developed 50 years ago (74, 75), have been equipped with cameras whose imaging system uses separate charge-coupled devices (3CCD) which capture the image of the microscopic field. The image recorded in the computer is displayed on a high-definition video monitor (76–80). Bone tissue is detected according to a selected color threshold and parameters of bone structure and

microarchitecture are automatically provided. In addition, interactive measurements of parameters reflecting the bone turnover can be also obtained (80, 81). The equipment now associates automatic and semi-automatic systems. The measurements of the different components of the bone tissue can be performed on a live image and traced directly on the computer screen with x - y positions of the enhanced live overlay linked to the motorized x - y stage. In addition, live image stitching makes it possible to obtain large mosaic-images that offer the advantage of a wide field and very high resolution.

Histomorphometric Parameters

Terminology

A standardization of the nomenclature for histomorphometric parameters was initially established by the ASBMR committee in 1987 (82) and updated in 2013 (31). The objective of this nomenclature is to clarify the terminology used in the past and gives the abbreviations which must be used in all bone histomorphometric studies. The principle is to express all data by using the same format, i.e., Source-Measurement/Referent where the source is the region (cortical (Ct), cancellous (Cn), endocortical (Ec), periosteal (Ps) bone, or total core (Tt)). All measurements must be expressed as an index of the amount of tissue analyzed which are mainly bone surface (BS), bone (BV) volume, or tissue (TV) volume of the region analyzed. Only the measurements of distance, i.e., width, can be given without referent. The data can be expressed in two-dimensional, e.g., width (Wi), perimeter (Pm) and area (Ar), or three-dimensional e.g., thickness (Th), surface (S) and volume (V), terminology, but only one type of terminology can be used in an article.

Parameters of Bone Resorption

The main problem in assessing bone resorption is to analyze a structure which has disappeared (**Table 1**). Eroded surfaces are identified by their irregular and crenated aspects with the presence of osteoclasts but resorption cavities may not be deep and without the presence of osteoclast. The identification of eroded lamellae under polarized light may help the characterization of lacunae (83). As previously mentioned, osteoclasts can be identified by the presence of tartrate resistant acid phosphatase. Erosion depth reflects the activity of osteoclasts. Different procedures to assess the erosion depth have been reported. The first one was based on the inverse relationship between erosion depth and the interstitial width, i.e., the distance between two BSU situated on opposite sides of a trabecula (84). However, this relationship is influenced by any changes of the wall width and trabecular thickness (85, 86). Other authors evaluated erosion depth by counting the number of eroded lamellae and measuring the thickness of lamellae (87). In addition, these authors separated eroded cavities according to the presence of osteoclasts, mononuclear, or preosteoblastic cells related to the stages of resorptive phase. This method depends on the ability to suitably identify these different cell types, only on their morphology. This method has never been used by other groups. A computerized method (88) and an interactive reconstruction approach (80) have been used to reconstruct the bone surface before the onset of the resorption. This method

TABLE 1 | Measured parameters reflecting the bone remodeling and mineralization.

Parameters	Abbreviations	Units
Osteoid surface	OS/BS	%
Osteoid volume	OV/BV	%
Osteoid thickness	O.Th	μm
Eroded surface	ES/BS	%
Erosion depth	E.De	μm
Eroded volume	EV/BV	%
Osteoclast surface	Oc.S/BS	%
Osteoclast number	Oc.N/BS	#/mm
Single labeled surface	sLS/BS	%
Double labeled surface	dLS/BS	%
Inter label distance	Ir.L.Th	μm

BS, bone surface; BV, bone volume.

allows only an estimation of the erosion depth (mean and maximum) and volume because measurements are performed independently of the resorption stage, including resorption cavities not totally achieved. Despite an underestimation of the erosion depth, a correlation has been found with deoxyypyridinoline, a marker of the bone resorption (80). A true final erosion depth has been obtained with a similar method applied only on cavities covered with a thin layer of osteoid, ensuring that the resorption has ended (89) but with this method there is a limit to the number of measurements that can be done.

Parameters of Bone Formation

Bone formation includes two stages, the first one is the matrix apposition by the osteoblasts followed, after a delay, by the mineralization process. They can be quantified by the static parameters of bone formation (**Table 1**) and by the dynamic parameters derived from the measurement of tetracycline labels (90) (**Table 2**). Activation frequency (Ac.f; #/year) is the probability that a new remodeling will appear at any point on the bone surface and represents the birthrate of a new remodeling site (91). Activation frequency is derived from parameters of formation while the activation of a remodeling results in resorption. A coupling between resorption and formation is required for a valid interpretation of activation frequency.

Parameters of Bone Structure

The bone mass and microarchitecture are major determinants of the bone strength and the measurements of cortical thickness and cancellous bone volume were two of the first parameters assessed (**Table 3**). In recent years, non-invasive imaging methods such as quantitative microcomputed tomography (microCT) or high-resolution peripheral quantitative computed tomography (HR-pQCT) provide three-dimensional structural parameters at peripheral sites (hip and spine) but these techniques detect only mineralized tissue. MicroCT can be also applied to bone samples allowing the measurement of 3-dimensional microarchitecture parameters. Most of the parameters obtained by non-invasive methods correlate with those measured by histomorphometry (93). However, due to the difference in resolution (80 μm for HR-pQCT and less 5 μm for histomorphometry), differences may be observed for a few parameters such as cortical porosity (94), as pores with a small diameter cannot be detected by microCT in contrast to histomorphometry.

The trabecular connectivity is another determinant of the bone strength. Parameters have been described including the strut analysis (76) and the evaluation of the spatial distribution of trabeculae, their connectivity, and complexity (42, 81, 95–97). Trabecular bone pattern factor (TbPF; #/mm) and Euler number provide an estimation of the trabecular bone connectivity and complexity and have been shown to correlate with bone strength independently to the bone quantity (98). Fractal dimension (FD) reflects the degree of complexity (99–102). The fractal dimension can be assessed on images acquired by radiography, microCT, and on histological sections. A correlation between the fractal dimension and mechanical properties of bone have been reported (103–105).

These microarchitecture parameters provide different and complementary informations on the trabecular network. They have been used until the development of microCT, and several microCT outcomes were derived from them, e.g., connectivity was derived from the Euler number (106).

Reproducibility of Bone Histomorphometry

Even when suitable methods have been applied, several factors can influence measurements as variations in the results may be observed between laboratories and few centers around the world

TABLE 2 | Derived histomorphometric parameters of bone remodeling and mineralization.

Parameters	Abbreviations	Formulae	Units
Mineralization rate	MAR	Ir.L.Th/Ir.L.t	μm/day
Mineralizing surface	MS/BS	((dLS+ sLS/2)/BS)	%
Bone formation rate	BFR/BS	MAR * MS/BS	μm ³ /μm ² /day
Activation frequency	Ac.f	(BFR/BS)/W.Th	#/yr
Adjusted appositional rate	Aj.AR	MAR/(MS/OS)	μm/day
Mineralization lag time	Mlt	O.Th/Aj.AR	days
Osteoid maturation time	Omt	O.Th/MAR	days
Formation period	FP	W.Th/Aj.AR	days
Active formation period	FPa+	W.Th/MAR	days
Quiescent period	QP	FP *(QS/OS)	days
Resorption period	Rs.P	FP *(Oc.S/OS)	days
Reversal period	Rv.S	FP *(ES-Oc.S/OS)	days

Ir.L.t, inter-labels time; W.Th, wall thickness; QS, quiescent surface.

TABLE 3 | Histomorphometric parameters of bone structure and microarchitecture.

Parameters	Abbreviations	Units
<i>Measured parameters</i>		
Cortical thickness	Ct.Th	μm
Cortical porosity	Ct.Po	%
Bone volume	BV/TV	%
Surface density	BS/BV	%
Wall thickness	W.Th	μm
<i>Derived parameters</i>		
Trabecular thickness*	Tb.Th	μm
Trabecular number	Tb.N	#/mm ²
Trabecular separation	Tb.Sp	μm

*An indirect evaluation of trabecular thickness can be calculated from area and perimeter which is based on a plate model (92).

have the equipment and expertise (107). For these reasons, the methods must be precisely described in manuscripts reporting histomorphometric studies. The main causes of these variations may be due to the sampling, laboratory processing, and measuring methods.

Inter-Sample Variation

Several studies investigated different locations of iliac biopsies as the iliac crest is not perfectly isotropic and the trabecular organization can vary between sites within the ilium (65). Even if some differences are observed between the left and right side (108–110) or between different localizations within iliac crest, they were not significant in a group of patients (109–113). However, in a single patient having repeated biopsies, these variations must be considered to affirm the efficacy of treatment (109, 110, 113) and to design the patient group size in clinical trials to detect significant differences when repeated biopsies are conducted (114). Within one core, the variance decreases when the number of microscopic fields and sections increase (115, 116). This points out the recommendation to use a trephine with a 7.5 mm inner diameter and to measure a total tissue area of at least 30 mm² (30, 31) on sections cut in 2–3 plans separated by 200–300 μm.

Laboratory Processing

Different staining dyes have been applied to differentiate osteoid and mineralized tissue. Despite significant correlations, some differences were reported between Masson trichrome and toluidine blue (111) or solochrome cyanin and trichrome (117). The measurement of distance may be also influenced by the thickness of the sections (66, 118) and the section obliquity during sectioning. They result in an apparent profile of the structure different from the true value and this variation depends on the thickness of the section and the angle from an ideal perpendicular section. For cortical sections, the projection error is negligible, regardless of the section thickness. For the other thickness measurements, the obliquity can be corrected by multiplying the measured values by $\pi/4$ (66).

Measuring Methods

Previous studies reported a good correlation between parameters measured by a manual point counting method and computerized

image analyzers (72, 73) with coefficients of correlation ranging from 0.90 to 0.98 (73). The variation between methods was found higher than the inter-observer variation (119). However, some variations may exist between different equipments requiring a validation procedure when a new equipment is acquired. It also points out the potential problems associated with the use of control data from other laboratories using different methods (119).

Inter-Observer Variation

Inter-observer variation may be important when measurements are performed by different laboratories using different techniques such as staining, magnification or measuring methods (119–121). It shows that it is difficult for one group to refer to the normal range established by another group without a previous cross-calibration. The experience of the observer is also a major factor of inter-observer variation (120). However, when measurements are performed by two experienced observers from the same group, inter-observer variation is lower than 6% (73, 115).

BONE BIOPSY AS A DIAGNOSIS TOOL

Initially, transiliac bone biopsy was widely used for the diagnosis of metabolic bone diseases, mainly osteoporosis. The main question was whether the iliac crest represents the entire skeleton, as the iliac crest is an unloading site without a high fracture risk. Relationships between the iliac bone and vertebrae were reported for the amount of bone and strength (122–125). A cancellous bone volume per tissue volume (Cn-BV/TV) lower than 11% was defined as the “vertebral fracture threshold” in osteoporotic patients (**Figure 3**) (126) and was used for many years as the reference value for the diagnosis of osteoporosis. Despite differences in microarchitecture and turnover between the iliac crest and the other skeletal sites, especially the sites prone to fracture as vertebra and femoral neck (127), significant correlations were found (95, 128) and age-related changes were observed in all sites (129). During the 1980s, the development of non-invasive methods, such as bone densitometry, allowed for the diagnosis of osteoporosis. However, bone histomorphometry remains the only method that allows the analysis of bone at the intermediary level of organization, i.e., the osteon in cortical bone and the bone structural unit in cancellous bone and to assess some key features, e.g., the mineralization or the bone texture.

Normative data for histomorphometric parameters, according to age and sex, have been established in most of histomorphometry laboratories (112, 130–139) which allows to conclude an abnormal bone remodeling, mineralization, and structure (140).

Presently, the main indications of bone biopsy are the diagnosis of osteomalacia, the characterization of renal osteodystrophy, or the investigation of bone fragility not responding to osteoporotic treatment to exclude a bone mastocytosis or any other rare causes of secondary

osteoporosis. Beside the quantitative analysis, qualitative observation of bone sections provides additional information as a normal lamellar or woven texture, the presence of microcallus, mineralization defects, and any abnormalities in the bone marrow.

Osteomalacia

Osteomalacia can be diagnosed on biochemical and radiological signs but bone biopsy is the only means to diagnose osteomalacia when these signs are not evident. Osteomalacia is characterized by osteoid accumulation with a thickening of osteoid seams associated with a decreased mineralization rate and an elongation of the mineralization lag time (141) (**Figure 4**). Double labels may be undetectable and appear diffused. A decreased mineralization rate alone is not specific of osteomalacia, it may be a sign of osteoblast activity diminution with a reduced matrix apposition. An increase in osteoid thickness with a normal mineralization rate may reflect an increased apposition rate (32). Osteomalacia is due to vitamin D deficiency but can also complicate chronic renal failure and be a consequence of aluminum intoxication in hemodialysis patients (142–144). Osteomalacia can also occur as a complication of previous gastric surgery, coeliac disease, or long-term parenteral nutrition (145). Recently, mineralization defects in jaw biopsies have been reported in bisphosphonate-treated patients suffering from an osteonecrosis of the jaw. Osteomalacia cannot be considered as the cause of osteonecrosis but may contribute to its development (146, 147).

Renal Osteodystrophy

Renal osteodystrophy is the bone manifestation of chronic kidney disease which may have different aspects. The first histological studies report that skeletal effects were both hyperparathyroidism and mineralization defects (148, 149). These bone abnormalities with the systemic disorders of

mineral and bone metabolism are designed by the term Chronic Kidney Disease-Mineral and Bone Disorder (CKD-MBD). Biochemical markers of formation and resorption and parathyroid hormone levels may help to determine the type of CKD-MBD but cross-sectional studies have shown some discrepancies between biomarkers and bone histology. The bone biopsy has been recognized as the gold standard for the diagnosis and classification for renal osteodystrophy (150, 151) and is recommended when there are inconsistencies among biochemical parameters, unexplained fractures, severe vascular calcifications, a suspicion of aluminum toxicity, or before bisphosphonate treatment (152). However, most nephrologists are reluctant to perform biopsies and the number of biopsies in renal insufficient patients remains insufficient. In these cases, the use of a smaller diameter trephine can provide information on the bone status. Renal osteodystrophy is classified according to the level of turnover, the mineralization, and the volume of bone (TMV classification). The predominant hyperparathyroid form is characterized by a marked increase in bone turnover with extended osteoid surface covered by osteoblasts, deep eroded surface with numerous osteoclasts, and an increase in labeled surfaces (**Figure 5A**). A fibrosis is often observed. The presence of thick osteoid seams with diffuse tetracycline labels signifies osteomalacia. In this latter form the turnover may be reduced (**Figure 5B**). Adynamic bone disease is characterized by a marked decrease of the bone turnover with absence of active bone formation or resorption and a low bone volume (**Figure 5C**). Mixed uremic osteodystrophy associates high turnover, mineralization defects and normal bone volume (152–154).

Bone Mastocytosis

Systemic mast cell disease is associated with either osteoporosis or osteosclerosis with possible skin lesions. When biological analyses suggests a mastocytosis, the bone biopsy allows for the

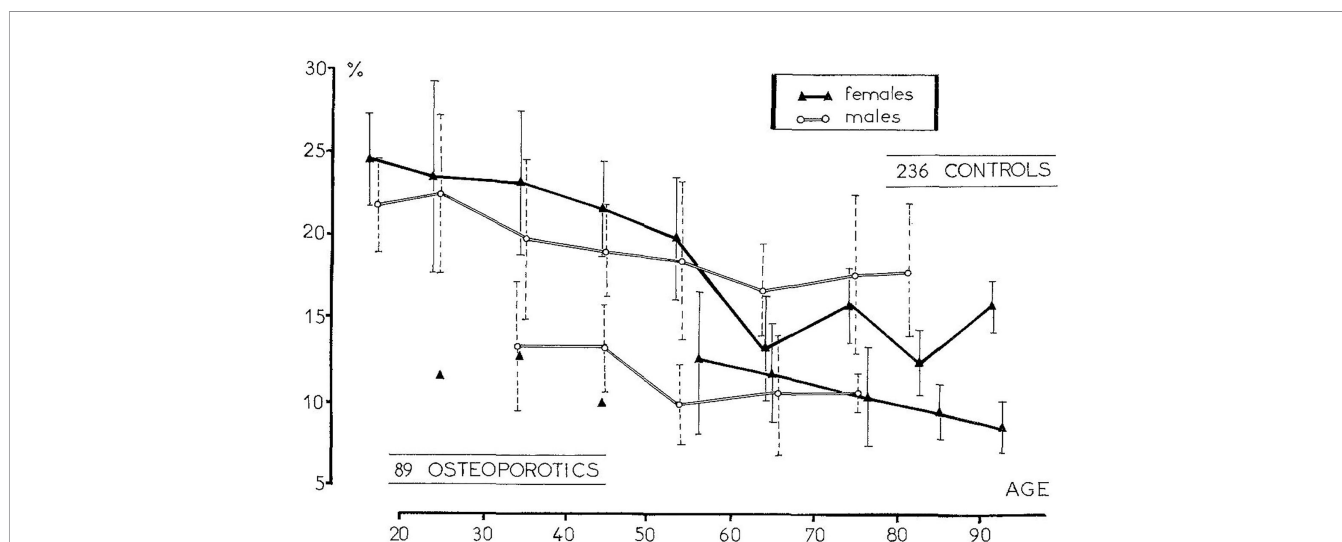


FIGURE 3 | The measurement of the trabecular bone volume in osteoporotic patients with one vertebral fracture allowed to define a “vertebral fracture threshold” at 11% [From Meunier et al. (126)].

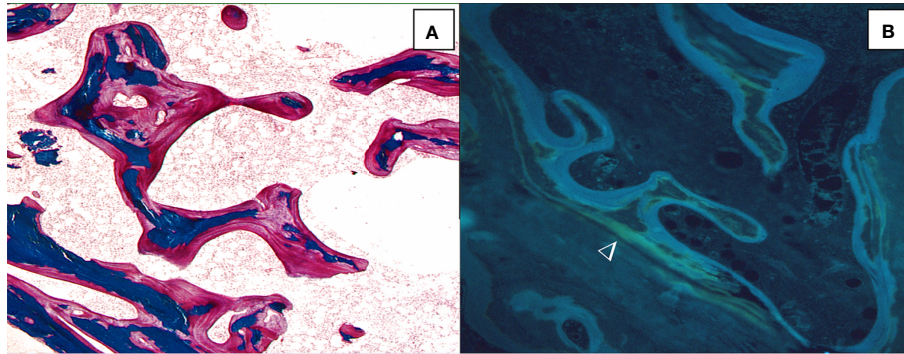


FIGURE 4 | Osteomalacia is characterized by thick and extended osteoid seams (A, solochrome cyanin R, x100) and diffuse tetracycline labels (▶) (B, unstained section under ultraviolet light; x100).

confirmation of an increased number of mast cells in the bone marrow. There has not been, however, a study that examined the sensitivity and specificity of the histologic analysis compared with tryptase measurement. An increased bone turnover is often reported with an unbalanced coupling between resorption and formation but without any mineralization defect (41, 155). Quantitative backscattered electron imaging showed a poorly mineralized bone in mastocytosis with osteosclerosis (156). The diagnosis is based on an increased number of mast cells in bone marrow, which may be close to the bone surface (Figure 2C). Mast cells are identified on bone sections stained with toluidine blue pH 2.6, May-Grünwald-Giemsa or acridine orange.

Endocrine Diseases

Bone fragility related to an alteration of the bone remodeling exists in several endocrine diseases such as hyperthyroidism and Cushing's syndrome (157). The high risk of fracture observed in acromegaly despite a normal BMD results from an alteration of the trabecular and cortical bone structure and architecture with a marked reduction of the osteoblasts number and activity (158).

BONE BIOPSY AS A RESEARCH TOOL

Initially, histomorphometric studies allowed for the characterization of bone diseases and osteoporosis appeared heterogeneous with different levels of remodeling (159, 160). The identification of high remodeling osteoporosis led to find endocrine disturbance such as primary hyperparathyroidism or hyperthyroidism (161). The analysis of bone biopsies also helped to understand the mechanism of remodeling, the coupling between resorption and formation, the process of mineralization, and thus, the pathogenesis of bone diseases (162). These studies showed that bone loss results from a negative balance at the bone structural unit, i.e., the amount of bone formed being lower than those previously resorbed, associated, or not with increased remodeling (163–165). The association of a high remodeling rate with deep resorption cavities produces a loss of trabecular plates. It may result in a

trabecular perforation that has a major deleterious effect on the bone strength (166) (Figure 6). However, further studies showed that bone loss is not the only cause of bone fragility (52). The development of techniques that can be applied to bone sections has allowed the assessment of the other components of the bone quality. Besides the amount of bone and the microarchitecture, the material composition of bone (collagen and mineral) and the accumulation of microdamages contribute to the bone strength. In addition to bone histomorphometric analysis, bone biopsy can be used to assay collagen crosslinks. A decrease in bone turnover is associated with an accumulation of pentosidine (167) which is negatively correlated with bone strength (168–170). Bone material's intrinsic properties can be analyzed by Fourier Transformed Infrared Microspectroscopy and the biomechanical behavior can be assessed by micro- or nano-indentation of bone samples (171, 172). All these components are controlled by the remodeling and any modifications of one of them result in bone fragility (157).

The coupling of osteoclasts and osteoblasts at the same remodeling site has been approached by the analysis of bone sections of hyperparathyroid patients showing that osteoclastic bone resorption and osteoblastic bone formation occur in a bone-remodeling compartments (BRC) (173). These authors observed that the canopy is separated from the bone marrow cavity by a monolayer of flat cells expressing osteoblast-like cell markers which is connected to capillaries. The contacts between these canopies and bone marrow capillaries initiate the bone remodeling (174).

During the past 30 years, basic and clinical studies have markedly enhanced the knowledge of the pathogenesis of bone diseases and especially on osteoporosis. The identification of molecules involved in the remodeling or the gene mutation in rare bone diseases have allowed for the development of new therapies (175). The magnitude of efficacy of new drugs is based on the fracture risk and bone mineral density but their approval requires a quantitative analysis of bone biopsies to assess their mechanisms of action at the tissue and cell level. Preclinical evaluations are firstly performed in animals, rodents, and large animals. However, especially in rodents, the histological

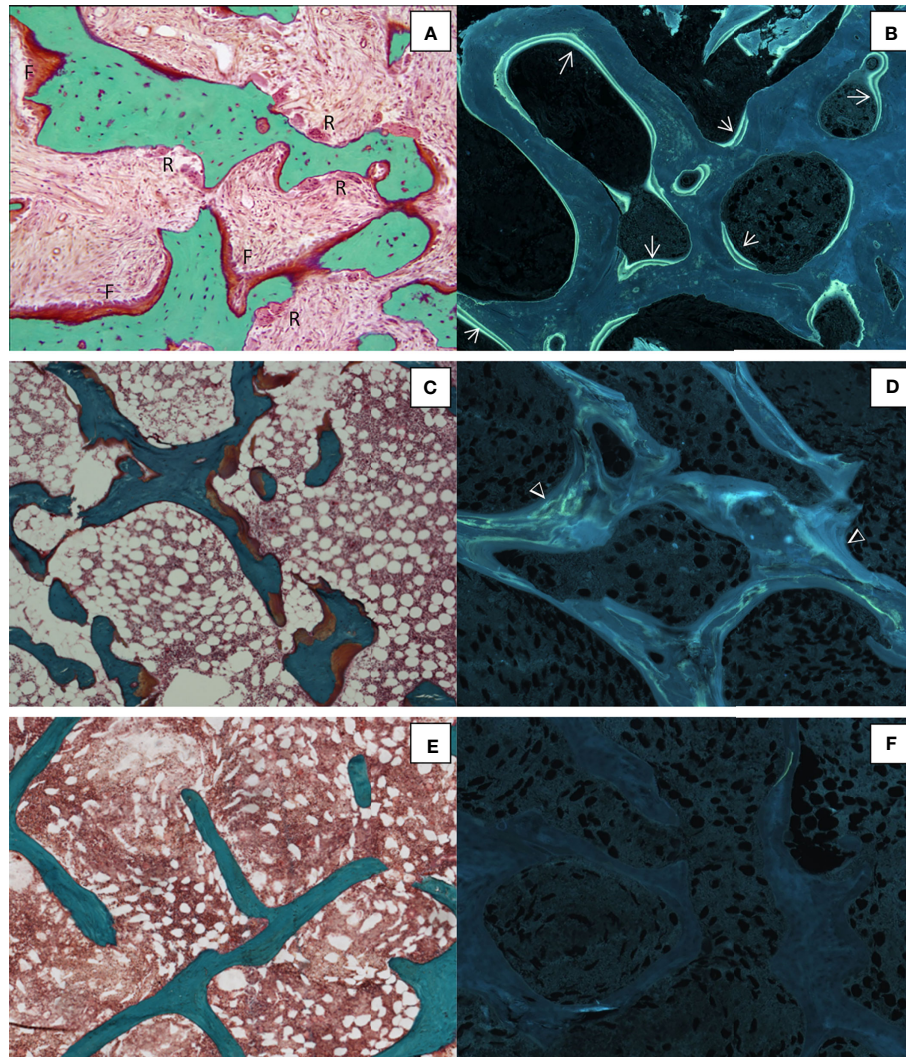


FIGURE 5 | Different histological forms of renal osteodystrophy. **(A)** High bone remodeling with increased bone resorption (R) and formation (F) associated with numerous tetracycline labels (→) **(B)**; Osteomalacia with thick osteoid seams **(C)** and diffuse tetracycline labels (Δ) **(D)**; Adynamic bone with no active bone surface **(E)** with no tetracycline label **(F)**. **(A, C, E)**, Goldner trichrome; **(B, D, F)**, unstained sections under ultraviolet light; x100.

procedures and the timing of double fluorochrome labeling must be adapted (176). Anti-osteoporotic treatments are divided in two main categories, inhibitors of the resorption and stimulators of bone formation.

Fluoride was one of the first treatments given in osteoporosis. High cumulative doses of fluoride induce a bone fluorosis which is characterized by a bone sclerosis due to an increased number of osteoblasts but with a toxic effect at the cell level (177) (**Figure 7**). Given at lower doses of 50 to 75 mg/day of sodium fluoride, it induced an increase in bone mass and osteoid parameters but also in mineralization defects (178–180). A marked decrease in trabecular bone quality was observed after long-term treatment (181). An abnormal mineral structure characterized by the presence of large crystals is present in newly formed bone which results in an increase in mineral density without improving the bone quality (182).

Bisphosphonates are synthetic analogues of pyrophosphate, with a phosphate-calcium-phosphate (PCP) bond. Many members of this class have been synthesized and divided into non-nitrogen-containing (etidronate, clodronate, tiludronate) and nitrogen-containing (pamidronate, alendronate, ibandronate, risedronate, zoledronate) bisphosphonates (183). Despite a different mechanism of action at the molecular level, and a different affinity to bone mineral, they strongly bind to hydroxyapatite crystals and inhibit the bone resorption (184). At the bone tissue level, the main effect of bisphosphonates is a marked decrease in the bone turnover. After 2 or 3 years, mineralizing surface and activation frequency decrease by 95% with alendronate (29), 80% with risedronate (185, 186), 73% with ibandronate (187), 91% with zoledronate (188) and 67% with pamidronate (189). Despite a marked decrease in the biochemical marker of bone resorption, no significant

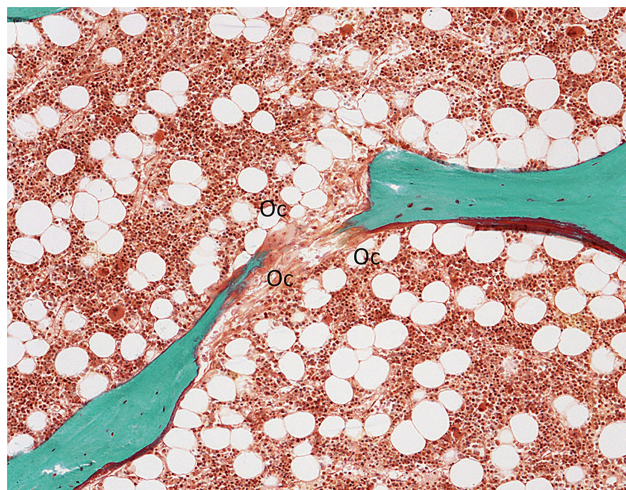


FIGURE 6 | Trabecular perforation due to osteoclastic (Oc) resorption. Goldner trichrome; x100.

reduction in eroded surface was reported (29, 185, 187, 188) which may be explained by a prolonged reversal phase. Due to the coupling between resorption and formation, a marked decrease in bone formation is also observed with no evidence of an increase in bone mass despite a marked increase in bone mineral density measured by DEXA. All these observations suggest an increased secondary mineralization related to the low turnover (190, 191). In summary, the consequence of the inhibitory effect of bisphosphonates on bone resorption is a decreased remodeling which results in a reduced remodeling space, a preservation of the cancellous bone microarchitecture with no change in bone mass, and an increase in bone mineral

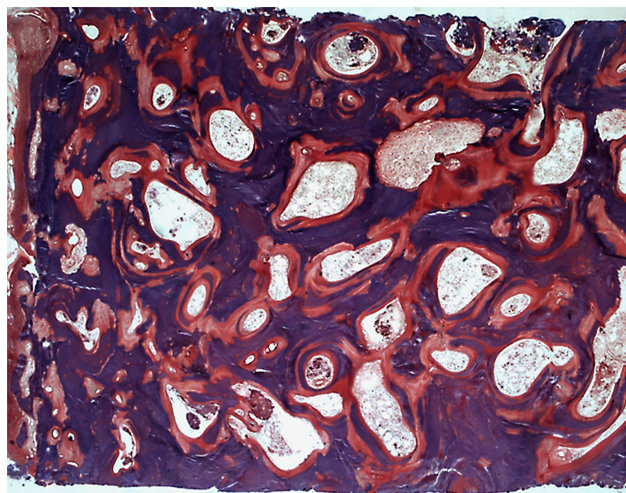


FIGURE 7 | Skeletal fluorosis characterized by an osteosclerosis with increased osteoid surfaces and mineralization defects in the trabeculae and around the osteocyte lacunae. Solochrome cyanin R; x50.

density. All these effects contribute to improve the bone strength. The marked decrease in bone turnover with bisphosphonates has been suggested to inhibit the repair of microcracks and favor their accumulations (192). An increased microcrack density has been observed in dogs receiving high doses of bisphosphonates (193) but this has not been confirmed in humans (194).

Selective estrogen receptor modulators (SERM) are compounds which have estrogen agonist actions in some tissues and estrogen antagonist actions on other tissues. In postmenopausal women, raloxifene induces a trend in decreased eroded surface, bone formation rate, and activation frequency. These results suggest that the effects of raloxifene on bone tissue are similar to estrogen (195).

Strontium ranelate was initially presented as an agent with a dual mechanism of action able to stimulate the formation and reduce the resorption. This assumption was supported by *in vitro* studies (196, 197) and preclinical investigations in rodents (198). However, in postmenopausal osteoporotic women, strontium ranelate does not significantly modify the parameters of bone formation or resorption after 1 to 3 years of treatment (199). A second large clinical trial confirmed the absence of significant increase in bone formation and the decrease of bone resorption at the bone tissue level (200), despite a significant improvement of the bone mineral density and fracture rate. A recent study reports decreases of crystallinity and carbonate content and the possibility that strontium may create bounds with collagenous and non-collagenous proteins but does not modify the nanomechanical properties (201).

The anabolic effect of parathyroid hormone in osteoporotic patients was reported in the mid-1970s (202, 203). The effect of intermittent administration of teriparatide, the fragment 1-34 of parathyroid hormone, varies according to the study. No significant increase in mineralizing surface and bone formation rate after 18 months (204) or a decrease between 6 and 18 months (205) of treatment have been reported. In contrast, significant increases in the formation and resorption were observed after 28 days and 2 years (206). Beside a classical remodeling-based formation, a contribution of a modeling-based formation has been proposed with intermittent PTH (1-34) administration (204, 206). In these studies, the criterion to identify modeling surfaces was the presence of smooth cement lines. Instead of the creation of new formative sites without prior resorption, an extended bone formation beyond the limit of the scalloped reversal line onto the adjacent quiescent surface has been suggested, i.e., an overflow from the remodeling surface rather than *de novo* modeling (21, 207, 208). Abaloparatide binds to the RG subtype of parathyroid hormone type 1 receptor with a higher affinity than teriparatide. No major difference in both static and dynamic histomorphometric variables have been observed between placebo, teriparatide, and abaloparatide (209). Nevertheless, compared to teriparatide, serum bone formation marker (sP1NP) decreases after 3 months and the increase in the resorption marker (sCTX) was lower with abaloparatide (210).

Odanacatib, an investigational agent previously in development, is a cathepsin K inhibitor which reduces bone

resorption *via* a mechanism distinct from other anti-resorptive drugs. Secretion of cathepsin K from the osteoclast results in degradation of type I collagen. The absence of cathepsin K activity in humans due to a CTSK mutation results in pycnodysostosis, a rare bone disease characterized by osteosclerosis and fractures (211, 212). Whereas other antiresorptive drugs decrease osteoclast activity or differentiation with a subsequent reduction in bone formation, odanacatib permits persistent osteoclast viability and activity and selectively inhibits the removal of matrix protein (213). At the bone tissue level, treatment with odanacatib did not change the dynamic parameters of bone formation and may increase the osteoclast number. An increased bone formation was observed at the periosteal surface contributing to the thickening of the cortices (214, 215). However, despite significant reduction of the fracture rate, odanacatib was ultimately withdrawn from the regulatory approval process after it was found to be associated with an increased risk of stroke.

Denosumab is a fully-human monoclonal antibody that binds receptor activator for nuclear factor κ B ligand (RANKL), an essential factor for osteoclast differentiation and activity. Denosumab binds and reversibly inhibits the activity of RANKL and, therefore, the formation, activity, and survival of osteoclasts. As an antiresorptive agent, denosumab treatment induces a marked reduction in bone remodeling with both a decreased resorption and consequently, a diminution of formation. These effects observed after 2 and 3 years (216) are maintained after extension of the treatment up to 5 (217) and 10 (218) years. However, in contrast to bisphosphonates which remain incorporated in bone until resorption occurs, the effects of denosumab are reversible after discontinuation (219). The decreased bone turnover results in an elongation of the secondary mineralization and thus, an augmentation of the degree of mineralization (218). In addition, a reduction of the endocortical erosion depth with no change of the mean wall thickness also contributes to the greater gain of BMD with denosumab than with other antiresorptive agents (220). The persistence of a modeling-based formation process has also been suggested (221); when the remodeling is very low, modeling bone formation may sparsely occur to preserve the bone mass (222), especially in loaded regions (223). A transient increase in endogenous PTH level after denosumab administration has been evoked (224) but not confirmed (225).

Romosozumab, a bone forming agent, is a humanized monoclonal antibody that binds and inhibits sclerostin, thereby, promoting osteoblast differentiation and activity. Sclerostin is a protein produced by osteocytes that inhibits the bone formation by inhibiting canonical Wnt signaling. Inherited sclerostin deficiency is characterized by a high bone mass (226). At the bone tissue level, romosozumab treatment induces an early and transient marked augmentation of bone formation parameters associated with a reduction of the resorption (22). This dual and opposite effect reflects a transient absence of coupling between resorption and formation. The occurrence of a modeling-based bone formation, previously reported in animal studies (227, 228), has been confirmed in humans (229). However, a self-regulatory

mechanism of the bone formation suggested by experimental studies (230) explains that later in treatment, only the decreased bone resorption remains associated with a decreased bone turnover as a consequence of the coupling. These effects result in an increased bone mass and improved microarchitecture. Romosozumab is the first anti-osteoporotic agent having both an anabolic and an antiresorptive action.

BONE HISTOMORPHOMETRY IN THE FUTURE

Computerized microscopy image analysis is widely used for diagnosis and prognosis in various fields of clinical practice and has improved the analysis of bone diseases. Recently, deep learning techniques have been developed (231) and applied in digital image processing (232), allowing for cell detection and classification (233). The application of these methods to bone histomorphometry will likely allow for easier diagnosis. The utility of machine learning based on biochemical testing, imaging, and clinical data has been reported in the diagnosis and fracture prediction in osteoporosis [see review (234)]. Combined with bone histomorphometry, the investigation of the molecular profile of circulating mesenchymal stem cells may provide information on the individual's osteogenic potential (151).

Many questions remain regarding the mechanism of coupling, the role of the reversal phase, and the several weeks separating the osteoclastic resorption and the osteoblastic formation (235–237). Numerous factors released during the resorption phase have been identified as playing a role in the coupling between resorption and formation. These factors may be released from the resorbed bone matrix, secreted by osteoclasts or transported by microvesicles (238, 239). But the initiation of remodeling is not only based on the levels of these different factors but also requires a determinant for a specific site where osteoclasts and osteoblasts will successively work (240). A bone-remodeling compartment (BRC) separated from the bone marrow cavity by a monolayer of flat cells from the osteoblast lineage has been described (173). The extent of this canopy over remodeling sites varies in several pathological situations and a reduced canopy surface is associated with a smaller extent of bone-forming surfaces (173). Bone loss in postmenopausal osteoporosis is associated with absences of canopy above formation and eroded surfaces. Furthermore, an accumulation of arrested reversal surface and a decreased extent of surface of formation with a modification of osteoblasts morphology from a cuboidal to flattened shape is observed (241). A loss of BRC canopies is also reported in multiple myeloma (242), Cushing's syndrome (243), and glucocorticoid-induced osteoporosis (244). In recent years, additional observations have been provided by the Delaisse group (245, 246). At the beginning of the reversal period, mononuclear cells remove the demineralized collagen before the onset of osteoblasts and the secretion of the bone matrix. These cells have been initially identified as macrophages but ultrastructural analysis showed

that they are bone lining cells able to activate matrix metalloproteinase (246). By analyzing 3D reconstruction of serial sections of Haversian systems in human long bone, these authors captured the events ranging from initiation of resorption to onset of formation as a functional continuum. They described a mixed “reversal-resorption” phase characterized by the presence of both osteoclasts and reversal/osteoprogenitor cells. The reversal/osteoprogenitor cells gradually matured into osteoblasts and bone formation is initiated only above a threshold cell density. The length of the reversal/resorption period depends on how fast osteoprogenitor recruitment reaches this threshold (247). The activation of remodeling is linked to the development of the vasculature close to the bone surface and this interaction between capillary and canopy provides osteoblasts progenitors (248). Based on these observations, an additional mechanism of alendronate has been recently reported where osteoprogenitors recruitment is slowed down on eroded surfaces and consequently, the onset of bone formation is delayed (249). These observations provide information to better understand how the balance between resorption and formation is regulated.

A better understanding of existing treatment is essential to improve their use. Over the past decades, studies have focused on the effects of new therapeutics for bone remodeling but forgot the process of modeling described more than 50 years ago (250). A modeling-based formation was firstly reported for teriparatide mainly due to an overflow of the remodeling surface (21). Denosumab strongly inhibits remodeling-based formation but little remaining modeling has been suggested (221). In contrast to other existing treatments, the early marked increase in bone formation with romosozumab results from a higher proportion of modeling than remodeling based formation (22, 229). Thus, from these observations, it appears that in addition to the remodeling, the modeling process may contribute to the antifracture efficacy of therapeutic agents and needs to be suitably assessed (251). Denosumab is an effective anti-osteoporotic agent but a rapid bone loss with an increased fracture risk is observed after treatment withdrawal, suggesting a rebound in osteoclast activity. McDonald et al. (252), using intra-vital imaging, observed a fission of osteoclasts into smaller motile cells named osteomorphs which were able to refuse and form osteoclasts in another site. Inhibition of RANKL by osteoprotegerin treatment results in the accumulation of osteomorphs able to rapidly fuse into active osteoclasts upon osteoprotegerin withdrawal. These observations may explain the

rebound after denosumab discontinuation. These findings will open new investigations on the pathogenesis and treatment of bone diseases.

SUMMARY AND CONCLUSION

The diagnosis of the majority of bone diseases is based on clinical, radiological, and biochemical examinations with the development of non-invasive methods as bone densitometry, biochemical markers, and quantitative computed tomography. Nevertheless, bone histomorphometry remains the only method for the study of bone at the tissue and cellular levels. Qualitative and quantitative analyses of transiliac bone biopsies require strict methodological conditions which have been initially described more than 60 years ago. Bone biopsy, which is an invasive method, has limited indicators for diagnostic purposes, especially in osteoporosis. The iliac crest being an unloading skeletal site, in contrast to the spine and the femoral neck which is prone to fracture is the only mean for diagnosing a mineralization defect. The recommended procedure is to collect a horizontal transiliac bone biopsy with a 7.5 mm inner diameter trephine. A previous fluorochrome double labeling is required to assess the mineralization and the dynamic of bone formation. For a better representation, sections are cut at 3 different levels and Goldner trichrome staining allows assessing both resorption and formation parameters. The progress of image analyzers, improved the analysis of bone sections, and the development of new image techniques will help the analysis of bone biopsy in the future. Bone histomorphometry will continue to play a major role in the understanding of the pathophysiology of metabolic bone diseases and the evaluation of the safety and mechanisms of action of therapeutics.

AUTHOR CONTRIBUTIONS

PC and RC contributed to the manuscript and approved the final version.

ACKNOWLEDGMENTS

The authors thank Jean Paul Roux for comments on the manuscript.

REFERENCES

1. Frost HM. *Bone Remodeling Dynamics*. Springfield, IL, USA: Charles C Thomas Company (1964). 175p.
2. Frost HM. Bone Dynamics in Metabolic Bone Disease. *J Bone Jt Surg* (1966) 48A:1192–203.
3. Frost HM. Tetracycline-Based Histological Analysis of Bone Remodeling. *Calcif Tissue Res* (1969) 3:211–37. doi: 10.1007/BF02058664
4. Frost HM. The Skeletal Intermediary Organization. *Metab Bone Dis Relat Res* (1983) 4(5):281–90. doi: 10.1016/s0221-8747(83)80001-0
5. Delesse M. Procédé Mécanique Pour Déterminer la Composition des Roches. In: *Compte-rendu de l'Académie des Sciences*. Paris (1847). p. 544–52.
6. Bordier P, Matrajt H, Miravet L, Hioco D. Mesure Histologique de la Masse Et de la Résorption des Travées Osseuses. *Path Biol* (1964) 12:1238–43.
7. Rao SD. Practical Approach to Bone Biopsy. In: RR Recker, editor. *Bone Histomorphometry. Techniques and Interpretation*. Boca Raton, FL, USA: CRC Press (1983). p. 3–12.
8. Visser WJ, Niermans HJ, Roelofs JMM, Raymakers JA, Duursma SA. Comparative Morphometry of Bone Biopsies Obtained by Two Different

- Methods From the Right and Left Iliac Crest. In: PJ Meunier, editor. *Bone Histomorphometry. Second International Workshop*. Paris, France: Armour Montagu (1976). p. 79–87.
9. Duncan H, Rao SD, Parfitt AM. Complications of Bone Biopsies. In: WSS Jee and AM Parfitt, editors. *Bone Histomorphometry 1980*. Paris, France: Amour Montagu (1980). p. 483–86.
 10. Shalton A, Michell PA, Betts JA, Darby AJ, Gishen P. Jamshidi Needle Biopsy of Bone Lesions. *Clin Radiol* (1982) 33:193–6. doi: 10.1016/s0009-9260(82)80061-5
 11. Faugere MC, Malluche HH. Comparison of Different Bone Biopsy Techniques for Qualitative and Quantitative Diagnosis of Metabolic Bone Diseases. *J Bone Jt Surg* (1983) 65a:1314–9.
 12. Jowsey J. *The Bone Biopsy*. Boston, MA, USA, Springer (1977).
 13. Visser WJ, Roelofs JMM, Duursma SA. Bone Density in the Iliac Crest. *Metab Bone Dis Rel Res* (1981) 3:187–90. doi: 10.1016/0221-8747(81)90007-2
 14. Ritz E, Malluche H, Krempien B, Mehls O. Bone Histology in Renal Insufficiency. In: DS David, editor. *Perspective in Nephrology and Hypertension*. New York, USA: John Wiley & Sons (1977). p. 197–233.
 15. Sun TC, Mori S, Roper J, Brown C, Hooser T, Burr DB. Do Different Fluorochrome Labels Give Equivalent Histomorphometric Information? *Bone* (1992) 13:443–6. doi: 10.1016/8756-3282(92)90088-e
 16. Pautke C, Vogt S, Kreutzer K, Haczek C, Wexel G, Kolk A, et al. Characterization of Eight Different Tetracycline: Advances in Fluorescence Bone Labelling. *J Anat* (2010) 217:76–82. doi: 10.1111/j.1469-7580.2010.01237.x
 17. Frost HM. Bone Histomorphometry: Choice of Marking Agent and Labeling Schedule. In: RR Recker, editor. *Bone Histomorphometry: Techniques and Interpretation*. Boca Raton, FL, USA: CRC Press (1983). p. 37–52.
 18. Harris WH, Travis DF, Friberg U, Radin E. The *In Vivo* Inhibition of Bone Formation by Alizarin Red S. *J Bone Joint Surg Am* (1964) 46:493–508.
 19. Parfitt AM, Foldes J, Villanueva AR, Shih MS. Difference in Label Length Between Demethylchlorotetracycline and Oxytetracycline: Implications for the Interpretation of Bone Histomorphometric Data. *Calcif Tissue Int* (1991) 48:74–7. doi: 10.1007/BF02555869
 20. Kunin CM, Finland M. Clinical Pharmacology of the Tetracycline Antibiotics. *Clin Pharmacol Ther* (1961) 2:51–69. doi: 10.1002/cpt19612151
 21. Lindsay R, Cosman F, Zhou H, Bostrom MP, Shen VW, Cruz JAD, et al. A Novel Tetracycline Labeling Schedule for Longitudinal Evaluation of the Short-Term Effects of Anabolic Therapy With a Single Iliac Crest Bone Biopsy: Early Actions of Teriparatide. *J Bone Miner Res* (2006) 21:366–73. doi: 10.1359/JBMR.051109
 22. Chavassieux P, Chapurlat R, Portero-Muzy N, Roux JP, Garcia P, Brown JP, et al. Bone-Forming and Antiresorptive Effects of Romosozumab in Postmenopausal Women With Osteoporosis: Bone Histomorphometry and microCT Analysis After 2 and 12 Months of Treatment. *J Bone Miner Res* (2019) 34:1597–608. doi: 10.1002/jbmr.3735
 23. Schenk RK, Olah AJ, Hermann W. Preparation of Calcified Tissues for Light Microscopy. In: GR Dickson, editor. *Methods of Calcified Tissue Preparation*. Amsterdam: Elsevier (1984). p. 1–56.
 24. Baron R, Vignery A, Neff L, Silverglate A, Santa Maria A. Processing of Undecalcified Bone Specimens for Bone Histomorphometry. In: RR Recker, editor. *Bone Histomorphometry: Techniques and Interpretation*. Boca Raton, FL, USA: CRC Press (1983). p. 13–35.
 25. Brinn NT, Pickett JP. Glycol Methacrylate for Routine Special Stains, Histochemistry, Enzyme Histochemistry and Immunohistochemistry. *J Histochemol* (1979) 3:125–30.
 26. Chappard D, Palle S, Alexandre C, Vico L, Riffat G. Bone Embedding in Pure Methyl Methacrylate at Low Temperature Preserves Enzyme Activities. *Acta Histochem* (1987) 81:183–97. doi: 10.1016/S0065-1281(87)80012-0
 27. Wolf E, Rösen K, Hahn M, Welkerling H, Dellling G. Enzyme and Immunohistochemistry on Undecalcified Bone and Bone Marrow Biopsies After Embedding in Plastic: A New Embedding Method for Routine Application. *Virchow Arch* (1992) 420:17–24. doi: 10.1007/BF01605979
 28. Erben RG. Embedding of Bone Samples in Methylmethacrylate: An Improved Method Suitable for Bone Histomorphometry, Histochemistry, and Immunohistochemistry. *J Histochem Cytochem* (1997) 45:307–13. doi: 10.1177/002215549704500215
 29. Chavassieux PM, Arlot MA, Reda C, Wei L, Yates AJ, Meunier PJ. Histomorphometric Assessment of the Long-Term Effects of Alendronate on Bone Quality and Remodeling in Patients With Osteoporosis. *J Clin Invest* (1997) 100:1475–80. doi: 10.1172/JCI119668
 30. Recker RR, Kimmel DB, Dempster D, Weinstein RS, Wronski TJ, Burr DB. Issues in Modern Bone Histomorphometry. *Bone* (2011) 49:955–64. doi: 10.1016/j.bone.2011.07.017
 31. Dempster DW, Compston JE, Drezner MK, Glorieux FH, Kanis JA, Malluche HH, et al. Standardized Nomenclature, Symbols and Units for Bone Histomorphometry. A 2012 Update of the Report of the ASBMR Histomorphometry Nomenclature Committee. *J Bone Miner Res* (2013) 28:2–17. doi: 10.1002/jbmr.1805
 32. Meunier PJ. Histomorphometry of the Skeleton. In: WA Peck, editor. *Bone and Mineral Research. Annual 1. A Yearly Survey of Developments in the Field of Bone and Mineral Metabolism*. Amsterdam, Oxford, Princeton: Excerpta Medica (1983). p. 191–222.
 33. Villanueva AR. Methods for Preparing and Interpreting Mineralized Sections of Bone. In: ZFG Jaworski, editor. *Proceedings of the First Workshop on Bone Morphometry*. Ottawa, Canada: University of Ottawa Press (1976). p. 341–53.
 34. Villanueva AR, Lundin KD. A Versatile New Mineralized Bone Stain for Simultaneous Assessment of Tetracycline and Osteoid Seams. *Stain Technol* (1989) 64:129–38. doi: 10.3109/10520298909106985
 35. Matrajt M, Hioco D. Solochrome Cyanin R as an Indicator Dye of Bone Morphology. *Stain Technol* (1966) 41:97–100. doi: 10.3109/10520296609116287
 36. Villanueva AR. A Bone Stain for Osteoid in Fresh, Unembedded, Mineralized Bone. *Stain Technol* (1974) 49:1–8. doi: 10.3109/10520297409116928
 37. Compston JE, Vedi S, Webb A. Relationship Between Toluidin Blue-Stained Calcification Fronts and Tetracycline Labelled Surface in Normal Human Iliac Crest Biopsies. *Calcif Tissue Int* (1985) 37:32–5. doi: 10.1007/BF02557675
 38. Goldner J. A Modification of the Masson Trichrome Technique for Routine Laboratory Purposes. *Am J Pathol* (1938) 14:247–9.
 39. Villanueva AR, Mehr L. Modifications of the Goldner and Gomori One-Step Trichrome Stains for Plastic Embedded Thin Sections of Bone. *Am J Med Technol* (1977) 43:536–8.
 40. Villanueva AR, Sypitkowski C, Parfitt AM. A New Method for Identification of Cement Lines in Undecalcified, Plastic Embedded Sections of Bone. *Stain Technol* (1986) 61:83–8. doi: 10.3109/10520298609110713
 41. Mey E, Roux JP, Buffet A, Edouard C, Meunier PJ. Bone Involvement in Systemic Mast Cell Disease (Abstract). *J Bone Miner Res* (1992) 7(Suppl. 1):S298. doi: 10.1002/jbmr.5650071104
 42. Chavassieux P, Arlot M, Meunier PJ. Clinical Use of Bone Biopsy. In: R Marcus, D Feldman and J Kelsey, editors. *Osteoporosis Second Edition Volume 2*. San Diego, CA, USA: Academic Press (2001). p. 501–9.
 43. Parsons V, Davies C, Goode C, Ogg C, Siddiqui J. Aluminium in Bone From Patients With Renal Failure. *Br Med J* (1971) 4:273–5. doi: 10.1136/bmj.4.5782.273
 44. Hellström HO, Mjoberg B, Mallmin H, Michaelsson K. The Aluminum Content of Bone Increases With Age, But is Not Higher in Hip Fracture Cases With and Without Dementia Compared to Controls. *Osteoporos Int* (2005) 16:1982–8. doi: 10.1007/s00198-005-1981-6
 45. Cournot-Witmer G, Zingraff J, Plachot JJ, Bourdeau A, Garabedian M, Escaig F, et al. Aluminum Localization in Bone From Hemodialyzed Patients: Relationship to Matrix Mineralization. *Kidney Int* (1981) 20:375–95. doi: 10.1038/ki.1981.149
 46. Maloney NA, Ott SM, Alfrey AC, Miller NL, Coburn JW, Sherrard DJ. Histological Quantitation of Aluminum in Iliac Bone From Patients With Renal Failure. *J Lab Clin Med* (1982) 99:206–16. doi: 10.5555/uri.pii0022214382900087
 47. Charhon SA, Chavassieux PM, Meunier PJ, Accominotti M. Serum Aluminium Concentration and Aluminium Deposits in Bone in Patients Receiving Haemodialysis. *Brit Med J* (1985) 290:1613–14. doi: 10.1136/bmj.290.6482.1613
 48. Walton JR, Diamond TH, Kumar S, Murrell GAC. A Sensitive Stain for Aluminum in Undecalcified Cancellous Bone. *J Inorg Biochem* (2007) 101:1285–90. doi: 10.1016/j.jinorgbio.2007.06.006

49. Chappard D, Alexandre C, Riffat G. Histochemical Identification of Osteoclasts. Review of Current Methods and Reappraisal of a Simple Procedure for Routine Diagnosis on Undecalcified Human Bone Biopsies. *Basic Appl Histochem* (1983) 27:75–85.
50. Chappard D, Palle S, Alexandre C, Vico L, Riffat G. Bone Embedding in Pure Methyl Methacrylate at Low Temperature Preserves Enzyme Activities. *Acta Histochem* (1987) 81:183–90. doi: 10.1016/S0065-1281(87)80012-0
51. Palle S, Chappard DL, Vico L, Riffat G, Alexandre C. Evaluation of The Osteoclastic Population in Iliac Crest Biopsies From 36 Normal Subjects: A Histoenzymologic and Histomorphometric Study. *J Bone Miner Res* (1989) 4:501–6. doi: 10.1002/jbmr.5650040408
52. Seaman E, Delmas PD. Bone Quality — The Material and Structural Basis of Bone Strength and Fragility. *N Engl J Med* (2006) 354:2250–61. doi: 10.1056/NEJMra053077
53. Frost HM. Presence of Microscopic Cracks *In Vivo* in Bone. *H Ford Hosp Med Bull* (1960) 8:27–35.
54. Lee TC, Mohsin S, Taylor D, Parkesh R, Gunnlaugsson T, O'Brien FJ, et al. Detecting Microdamage in Bone. *J Anat* (2003) 203:161–72. doi: 10.1046/j.1469-7580.2003.00211.x
55. Chapurlat RD, Delmas PD. Bone Microdamage: A Clinical Perspective. *Osteoporos Int* (2009) 20:1299–308. doi: 10.1007/s00198-009-0899-9
56. Zarrinkalam KH, Kuliwaba JS, Martin RB, Wallwork MAB, Fazzalari NL. New Insights Into the Propagation of Fatigue Damage in Cortical Bone Using Confocal Microscopy and Chelating Fluorochromes. *Eur J Morphol* (2005) 42:81–90. doi: 10.1080/09243860500096206
57. Portero-Muzy NR, Chavassieux PM, Arlot MA, Chapurlat RD. Staining Procedure for the Detection of Microcracks: Application to Ewe Bone. *Bone* (2011) 49:17–919. doi: 10.1016/j.bone.2011.07.001
58. Bain SD, Impeduglia TM CT. Cement Line Staining in Undecalcified Thin Sections of Cortical Bone. *Stain Technol* (1990) 65:159–63. doi: 10.3109/10520299009108065
59. Frost M, Rahbek ET, Ejersted C, Høilund-Carlsen PF, Bygum A, Thomsen JS, et al. Modeling-Based Bone Formation Transforms Trabeculae to Cortical Bone in the Sclerotic Areas in Buschke-Ollendorff syndrome. A Case Study of Two Females With LEMD3 Variants. *Bone* (2020) 135:115313. doi: 10.1016/j.bone.2020.115313
60. Weibel ER, Kistler GS, Scherle WF. Practical Stereological Methods for Morphometric Cytology. *J Cell Biol* (1966) 30:23–38. doi: 10.1083/jcb.30.1.23
61. Underwood EE. *Quantitative Stereology. 2nd ed.* Reading, MA, USA: Addison-Wesley Publishing Company (1970). 275p.
62. Elias H, Henning A, Schwatz DE. Stereology: Applications to Biomedical Research. *Physiol Rev* (1971) 51:158–200. doi: 10.1152/physrev.1971.51.1.158
63. Digabel H. Principles of Stereology in Bone Studies. In: ZFG Jaworski, editor. *Proceedings of the First Workshop on Bone Morphometry*. Ottawa, Canada: University of Ottawa Press (1973). p.16–20.
64. Howard V, Reed M. *Unbiased Stereology. Three Dimensional Measurements in Microscopy. Second Edition.* New-York, USA: Garland Science/BIOS Scientific Publishers (2005). 277p.
65. Whitehouse WJ. The Quantitative Morphology of Anisotropic Trabecular Bone. *J Microsc* (1974) 101:153–68. doi: 10.1111/j.1365-2818.1974.tb03878.x
66. Parfitt AM. The Stereologic Basis of Bone Histomorphometry. *Theory of Quantitative Microscopy and Reconstruction of the third Dimension*. In: RR Recker, editor. *Bone Histomorphometry: Techniques and Interpretation*. Boca Raton, FL, USA: CRC Press (1983). p. 53–87.
67. Frost HM. Human Haversian System Measurements. *Henry Ford Hosp Med Bull* (1961) 9:145–47.
68. Schenk R. Basic Stereological Principles. In: ZFG Jaworski, editor. *Proceedings of the First Workshop on Bone Morphometry*. Ottawa, Canada: University of Ottawa Press (1983). p. 21.
69. Braddley AJ, Gundersen HJG, Cruze Orive LM. Estimation of Surface Area From Vertical Sections. *J Microsc* (1986) 142:259–76. doi: 10.1111/j.1365-2818.1986.tb04282.x
70. Vesterby A, Kragstrup J, Gundersen HJG, Melsen F. Unbiased Stereology Estimation of Surface Density in Bone Using Vertical Sections. *Bone* (1987) 8:13–7. doi: 10.1016/8756-3282(87)90126-8
71. Manaka RC, Malluche HH. A Program Package of the Quantitative Analysis of Histologic Structure and Remodeling Dynamics of Bone. *Comp Prog BioMed* (1981) 13:191–201. doi: 10.1016/0010-468x(81)90098-2
72. Malluche HH, Sherman D, Meyer W, Massry SG. A New Semiautomatic Method for Quantitative Static and Dynamic Bone Histology. *Calcif Tissue Res* (1982) 34:439–48. doi: 10.1007/BF02411282
73. Chavassieux PM, Arlot MA, Meunier PJ. Intermethod Variation in Bone Histomorphometry: Comparison Between Manual and Computerized Methods Applied to Iliac Bone Biopsies. *Bone* (1985) 6:221–29. doi: 10.1016/8756-3282(85)90004-3
74. Meunier PJ. Use of an Image Analysing Computer for Bone Morphometry. In: AW Norman, K Schaefer, HG Grigoleit, DV Herrath and E Ritz, editors. *Clinical Aspects of Metabolic Bone Disease*. Amsterdam, The Netherlands: Excerpta Medica, Amsterdam (1973). p. 148–51.
75. McQueen CM, Smith DA, Monk IB, Horton PW. A Television Scanning System for the Measurement of the Spatial Variation of Micro-Density in Bone Sections. *Calcif Tiss Res* (1973) 11:124–32. doi: 10.1007/BF02547295
76. Garrahan NJ, Mellish RWE, Compston JE. A New Method for the Analysis of Two-Dimensional Trabecular Bone Structure in Human Iliac Crest Biopsies. *J Microsc* (1986) 142:341–9. doi: 10.1111/j.1365-2818.1986.tb04289.x
77. Huffer WE, Lepoff RB. An Indirect Method of Measuring Widths Suitable for Automated Bone Histomorphometry. *J Bone Miner Res* (1992) 7:1417–27. doi: 10.1002/jbmr.5650071209
78. Aaron JE, Johnson DR, Kanis JA, Oakley BA, O'Higgins P, Paxton SK. An Automated Method for the Analysis of Trabecular Bone Structure. *Comput Biomed Res* (1992) 25:1–16. doi: 10.1016/0010-4809(92)90031-5
79. Compston JE, Garrahan NJ, Croucher PI, Yamaguchi K. Quantitative Analysis of Trabecular Bone Structure. *Bone* (1993) 14:187–92. doi: 10.1016/8756-3282(93)90139-2
80. Roux JP, Arlot MA, Gineyts E, Meunier PJ, Delmas PD. Automatic-Interactive Measurement of Resorption Cavities in Transiliac Bone Biopsies and Correlation With Deoxyypyridinoline. *Bone* (1995) 17:153–56. doi: 10.1016/s8756-3282(95)00174-3
81. Portero NR, Arlot ME, Roux JP, Duboeuf F, Chavassieux PM, Meunier PJ. Evaluation and Development of Automatic Two-Dimensional Measurements of Histomorphometric Parameters Reflecting Trabecular Bone Connectivity: Correlations With Dual-Energy X-Ray Absorptiometry and Quantitative Ultrasound in Human Calcaneum. *Calcif Tissue Int* (2005) 77:195–204. doi: 10.1007/s00223-004-1260-0
82. Parfitt AM, Drezner MK, Glorieux FH, Kanis JA, Malluche H, Meunier PJ, et al. Bone Histomorphometry: Standardization of Nomenclature, Symbols, and Units. Report of the ASBMR Histomorphometry Nomenclature Committee. *J Bone Miner Res* (1987) 2:595–610. doi: 10.1002/jbmr.5650020617
83. Vedi S, Tighe JR, Compston JE. Measurements of Total Resorption Surface in Iliac Crest Trabecular Bone Inn Man. *Metab Bone Rel Res* (1984) 5:275–80. doi: 10.1016/0221-8747(84)90014-6
84. Courpron P, Lepine P, Arlot M, Lips P, Meunier PJ. Mechanisms Underlying the Reduction With Age of the Mean Wall Thickness of Trabecular Basic Structure Unit (BSU) in Human Iliac Bone. *Metab Bone Dis Rel Res* (1980) 2, Suppl:323–29.
85. Croucher PI, Mellish RWE, Vedi S, Garrahan NJ, Compston JE. The Relationship Between Resorption Depth and Mean Interstitial Bone Thickness: Age-Related Changes in Man. *Calcif Tissue Int* (1989) 45:15–9. doi: 10.1007/BF02556655
86. Parfitt AM, Foldes J. The Ambiguity of Interstitial Bone Thickness: A New Approach to the Mechanism of Trabecular Thinning. *Bone* (1991) 12:119–22. doi: 10.1016/8756-3282(91)90010-g
87. Eriksen EF, Gundersen HJG, Melsen F, Mosekilde L. Reconstruction of the Resorptive Site in Iliac Trabecular Bone; a Kinetic Model for Bone Resorption in 20 Normal Individuals. *Metab Bone Dis Rel Res* (1984) 5:235–42. doi: 10.1016/0221-8747(84)90065-1
88. Garrahan NJ, Croucher P, Compston JE. A Computerized Technique for the Quantitative Assessment of Resorption Cavities in Trabecular Bone. *Bone* (1990) 11:241–46. doi: 10.1016/8756-3282(90)90076-b
89. Cohen-Solal ME, Shih M-S, Lundy MW, Parfitt AM. A New Method for Measuring Cancellous Bone Erosion Depth: Application to the Cellular

- Mechanisms of Bone Loss in Postmenopausal Osteoporosis. *J Bone Miner Res* (1991) 6:1331–8. doi: 10.1002/jbmr.5650061210
90. Frost HM. Bone Histomorphometry: Analysis of Trabecular Bone Dynamics. In: RR Recker, editor. *Bone Histomorphometry: Techniques and Interpretation*. Boca Raton, FL, USA; CRC Press (1983). p. 109–31.
 91. Parfitt AM. The Physiologic and Clinical Significance of Bone Histomorphometric Data. In: RR Recker, editor. *Bone Histomorphometry: Techniques and Interpretation*. Boca Raton, FL, USA; CRC Press (1983). p. 143–223.
 92. Parfitt AM, Mathews CH, Villanueva AR, Kleerekoper M, Frame B, Rao DS. Relationships Between Surface, Volume, and Thickness of Iliac Trabecular Bone in Aging and in Osteoporosis. Implications for the Microanatomic and Cellular Mechanisms of Bone Loss. *J Clin Invest* (1983) 72:1396–409. doi: 10.1172/JCI111096
 93. Cohen A, Dempster DW, Müller R, Guo XE, Nickolas TL, Liu XS, et al. Assessment of Trabecular and Cortical Architecture and Mechanical Competence of Bone by High-Resolution Peripheral Computed Tomography: Comparison With Transiliac Bone Biopsy. *Osteoporos Int* (2010) 21:263–73. doi: 10.1007/s00198-009-0945-7
 94. Boutroy S, Vilaythiou N, Roux JP, Delmas PD, Blain H, Chapurlat RD, et al. Comparison of 2D and 3D Microarchitecture Evaluation at the Femoral Neck, Among Postmenopausal Women With Hip Fracture or Hip Osteoarthritis. *Bone* (2011) 49:1055–61. doi: 10.1016/j.bone.2011.07.037
 95. Chappard D, Basle M-F, Legrand E, Audran M. Trabecular Bone Microarchitecture: A Review. *Morphologie* (2008) 92:162–70. doi: 10.1016/j.morpho.2008.10.003
 96. Mellish RWE, Ferguson-Pell MW, Cochran GVB, Lindsay R, Dempster DW. A New Manual Method for Assessing Two-Dimensional Cancellous Bone Structure: Comparison Between Iliac Crest and Lumbar Vertebra. *J Bone Miner Res* (1991) 6:689–96. doi: 10.1002/jbmr.5650060706
 97. Compston J. Bone Histomorphometry. In: D Feldman, F Glorieux and Pike, editors. *Vitamin D*. Cambridge, MA, USA: Academic Press (1997). p. 573–86.
 98. Portero-Muzy NR, Chavassieux PM, Mitton D, Duboeuf F, Delmas PD, Meunier PJ. Euler_{strut.cavity}, a New Histomorphometric Parameter of Connectivity Reflects Bone Strength and Speed of Sound in Trabecular Bone From Human Os Calcis. *Calcif Tissue Int* (2007) 81:92–8. doi: 10.1007/s00223-007-9044-y
 99. Cutting JE, Garvin JJ. Fractal Curve, and Complexity. *Percept Psychophys* (1987) 42:365–70. doi: 10.3758/bf03203093
 100. Majumdar S, Weinstein RS, Prasad RR. Application of Fractal Geometry Techniques to the Study of Trabecular Bone. *Med Phys* (1993) 20:1611–19. doi: 10.1118/1.596948
 101. Majumdar S, Lin J, Link T, Millard J, Augat P, Ouyang X, et al. Fractal Analysis of Radiographs: Assessment of Trabecular Bone Structure and Prediction of Elastic Modulus and Strength. *Med Phys* (1999) 26:1330–40. doi: 10.1118/1.598628
 102. Fazzalari NL, Parkinson IH. Fractal Dimension and Architecture of Trabecular Bone. *J Pathol* (1996) 178:100–5. doi: 10.1002/(SICI)1096-9896(199601)178:1<100::AID-PATH429>3.0.CO;2-K
 103. Weinstein RS, Majumdar S. Fractal Geometry and Vertebral Compression Fractures. *J Bone Miner Res* (1994) 11:1797–802. doi: 10.1002/jbmr.5650091117
 104. Sanchez-Molina D, Velazquez-Ameijide J, Quintana V, Arregui-Dalmases C, Crandall JR, Subit D, et al. Fractal Dimension and Mechanical Properties of Human Cortical Bone. *Med Eng Phys* (2013) 35:576–82. doi: 10.1016/j.medengphy.2012.06.024
 105. Bauer JS, Kohlmann S, Eckstein F, Mueller D, Lochmüller E-M, Link TM. Structural Analysis of Trabecular Bone of the Proximal Femur Using Multislice Computed Tomography: A Comparison With Dual X-Ray Absorptiometry for Predicting Biomechanical Strength *In Vitro*. *Calcif Tissue Int* (2006) 78:78–89. doi: 10.1007/s00223-005-0070-3
 106. Odgaard A, Gundersen HJ. Quantification of Connectivity in Cancellous Bone, With Special Emphasis on 3-D Reconstructions. *Bone* (1993) 14:173–82. doi: 10.1016/8756-3282(93)90245-6
 107. Frost HM. The Numerical and Statistical Approach. In: ZFG Jaworski, editor. *Bone Morphometry*. Ottawa, Canada: University of Ottawa Press (1976). p. 24–34.
 108. Visser WJ, Roelofs JMM, Peters JJP, Lentferink MHF and Duursma SA. Sampling Variation in Bone Histomorphometry. *Metab Bone Dis Rel Res* (1980) 2 Suppl:429–34.
 109. De Vernejoul MC, Kuntz D, Miravet L, Goutallier D, Ryckewaert A. Bone Histomorphometry Reproducibility in Normal Patients. *Calcif Tissue Int* (1981) 33:369–74. doi: 10.1007/BF02409458
 110. Parisien MV, McMahon D, Pushparaj N, Dempster DW. Trabecular Architecture in Iliac Crest Bone Biopsies: Intra-Individual Variability in Structural Parameters and Changes With Age. *Bone* (1988) 9:289–95. doi: 10.1016/8756-3282(88)90012-9
 111. Melsen F, Melsen B, Mosekilde L. An Evaluation of the Quantitative Parameters Applied in Bone Histology. *Acta Path Microbiol Scand Sect A* (1978) 86:63–9. doi: 10.1111/j.1699-0463.1978.tb02013.x
 112. Malluche HH, Meyer W, Sherman D, Massry SG. Quantitative Bone Histology in 84 Normal American Subjects. Micromorphometric Analysis and Evaluation of Variance in Iliac Bone. *Calcif Tissue Int* (1982) 34:449–55. doi: 10.1007/BF02411283
 113. Chavassieux PM, Arlot ME, Meunier PJ. Intersample Variation in Bone Histomorphometry: Comparison Between Parameters Value Measured on Two Contiguous Transiliac Bone Biopsies. *Calcif Tissue Int* (1985) 37:345–50. doi: 10.1007/BF02553699
 114. Hauge EM, Mosekilde L, Melsen F, Frydenberg M. How Many Patients are Needed? Variation and Design Considerations in Bone Histomorphometry. *Bone* (2001) 28:556–62. doi: 10.1016/s8756-3282(01)00424-0
 115. Birkenhager-Frenkel DH, Schmitz PIM, Breuls PNWM, Lockefeller JHM, van der Heul RO. Biological Variation as Compared to Inter-Observer Variation and Intrinsic Error of Measurement, for Some Parameters, Within Single Bone Biopsies. In: PJ Meunier, editor. *Bone Histomorphometry. Second International Workshop*. Paris: Armour Montagu (1976). p. 63–7.
 116. Bonucci E, Ballanti P, Della Rocca C, Milani S, Lo Cascio V, Imbimbo B. Technical Variability of Bone Histomorphometric Measurements. *Bone Miner* (1990) 11:177–86. doi: 10.1016/0169-6009(90)90057-m
 117. Revel PA. Histomorphometry of Bone. *J Clin Pathol* (1983) 36:1323–31. doi: 10.1136/jcp.36.12.1323
 118. Birkenhager-Frenkel DH, Birkenhager JC. Bone Appositional Rate and Percentage of Doubly and Singly Labeled Surfaces: Comparison of Data From 5 and 20 µm Sections. *Bone* (1987) 8:7–12. doi: 10.1016/8756-3282(87)90125-6
 119. Wright CDP, Vedi S, Garrahan NJ, Stanton M, Duffy SW, Compston JE. Combined Inter-Observer and Inter-Method Variation in Bone Histomorphometry. *Bone* (1992) 13:205–8. doi: 10.1016/8756-3282(92)90198-6
 120. Delling G, Luehmann H, Baron R, Mathews CHE, Olah A. Investigation of Intra- and Inter-Reader Reproducibility. *Metab Bone Dis Rel Res* (1980) 2 Suppl:419–27.
 121. Compston JE, Vedi S, Stellan AJ. Inter-Observer and Intra-Observer Variation in Bone Histomorphometry. *Calcif Tissue Int* (1986) 38:67–70. doi: 10.1007/BF02556831
 122. Bell GH, Dunbar O. Variation in Strength of Vertebrae With Age and Their Relation to Osteoporosis. *Calc Tiss Res* (1967) 1:75–86. doi: 10.1007/BF02008077
 123. Melsen F, Vidik A, Melsen B, Mosekilde L. Some Relations Between Bone Strength, Ash Weight and Histomorphometry. In: PJ Meunier, editor. *Bone Histomorphometry Second International Workshop*. Paris: Armour Montagu (1976). p. 89–95.
 124. Podenphant J, Gotfredsen A, Nilas L, Nørgaard H, Brændstrup O. Iliac Crest Biopsy: Representativity for the Amount of Mineralized Bone. *Bone* (1986) 7:427–30. doi: 10.1016/8756-3282(86)90002-5
 125. Mosekilde L, Mosekilde L. Iliac Crest Trabecular Bone Volume as Predictor for Vertebral Compressive Strength, Ash Density and Trabecular Bone Volume in Normal Individuals. *Bone* (1988) 9:195–9. doi: 10.1016/8756-3282(88)90030-0
 126. Meunier P, Courpron P, Edouard E, Bernard J, Bringuier J, Vignon G. Physiological Senile Involution and Pathological Rarefaction of Bone. *Clin Endocrinol Metab* (1973) 2:239–56. doi: 10.1016/s0300-595x(73)80042-8
 127. Eventov I, Frisch B, Cohen Z, Hammel I. Osteopenia, Hematopoiesis, and Bone Remodelling in Iliac Crest and Femoral Biopsies: A Prospective Study

- of 102 Cases of Femoral Neck Fractures. *Bone* (1991) 12:1–6. doi: 10.1016/8756-3282(91)90047-m
128. Amling M, Herden S, Pöls M, Hahn M, Rtzel H, Delling G. Heterogeneity of the Skeleton: Comparison of the Trabecular Architecture of the Spine, the Iliac Crest, the Femur, and the Calcaneum. *J Bone Miner Res* (1996) 11:36–45. doi: 10.1002/jbmr.5650110107
 129. Thomsen JS, Ebbesen EN, Mosekilde LI. Static Histomorphometry of Human Iliac Crest and Vertebral Trabecular Bone: A Comparative Study. *Bone* (2002) 30:267–74. doi: 10.1016/s8756-3282(01)00666-4
 130. Meunier P, Courpron P. Iliac Trabecular Bone Volume in 236 Controls. Representativeness of Iliac Samples. In: ZFG Jaworski, editor. *Proceedings of the First Workshop on Bone Morphometry*. Ottawa, Canada: University of Ottawa Press (1973). p.100–5.
 131. Meunier P, Edouard C, Courpron P. Morphometric Analysis of Trabecular Resorption Surfaces in Normal Iliac Bone. In: ZFG Jaworski, editor. *Proceedings of the First Workshop on Bone Morphometry*. Ottawa, Canada: University of Ottawa Press (1973);p.156–60.
 132. Meunier P, Edouard C. Quantification of Osteoid Tissue in Trabecular Bone. Methodology and Results in Normal Iliac Bone. In: ZFG Jaworski, editor. *Proceedings of the First Workshop on Bone Morphometry*. Ottawa, Canada: University of Ottawa Press (1973). p. 191–6.
 133. Melsen B, Melsen B, Mosekilde L, Bergman S. Histomorphometric Analysis of Normal Bone From the Iliac Crest. *Acta Path Microbiol Scand Sect A* (1978) 86:70–81. doi: 10.1111/j.1699-0463.1978.tb02014.x
 134. Vedi S, Compston JE, Webb A, Tighe JR. Histomorphometric Analysis of Bone Biopsies From the Iliac Crest of Normal British Subjects. *Metab Bone Dis Rel Res* (1982) 4:231–6. doi: 10.1016/0221-8747(82)90032-7
 135. Vedi S, Compston JE, Webb A, Tighe JR. Histomorphometric Analysis of Dynamic Parameters of Trabecular Bone Formation in the Iliac Crest of Normal British Subjects. *Metab Bone Dis Rel Res* (1983) 5:69–74. doi: 10.1016/0221-8747(83)90004-8
 136. Rehman MTA, Hoyland JA, Denton J, Freemont AJ. Age Related Histomorphometric Changes in Bone in Normal British Men and Women. *J Clin Pathol* (1994) 47:529–34. doi: 10.1136/jcp.47.6.529
 137. Clarke BL, Ebeling PR, Jones JD, Wahner HW, O'fallon WM, Riggs BL, et al. Changes in Quantitative Bone Histomorphometry in Aging Healthy Men. *J Clin Endocrinol Metab* (1996) 81:2264–70. doi: 10.1210/jcem.81.6.8964862
 138. Glorieux FH, Travers R, Taylor A, Bowen JR, Rauch F, Norman M, et al. Normative Data for Iliac Bone Histomorphometry in Growing Children. *Bone* (2000) 26:103–9. doi: 10.1016/s8756-3282(99)00257-4
 139. Recker RR, Akhter MP, Lappe JM, Watson P. Bone Histomorphometry in Transiliac Biopsies From 48 Normal Healthy Men. *Bone* (2018) 111:109–15. doi: 10.1016/j.bone.2018.03.019
 140. Parfitt AM. The Physiologic and Pathogenic Significance of Bone Histomorphometric Data. In: FL Coe and MJ Favus, editors. *Disorders of Bone and Mineral Metabolism*. New York, USA: Raven Press (1992). p. 475–89.
 141. Parfitt AM. Osteomalacia and Related Disorders. In: LV Avioli and SM Krane, editors. *Metabolic Bone Disease, 3rd edition*. San Diego, CA: Academic Press (1998). p. 345–86.
 142. Hodsman AB, Sherrard DJ, Alfrey AC, Ott S, Brickman AS, Miller NL, et al. Bone Aluminum and Histomorphometric Features of Renal Osteodystrophy. *J Clin Endocrinol Metab* (1982) 54:539–46. doi: 10.1210/jcem-54-3-539
 143. Charhon SA, Chavassieux PM, Chapuy MC, Traeger J, Meunier P. Case Report: High Bone Turnover Associated With an Aluminum-Induced Impairment of Bone Mineralization. *Bone* (1986) 7:319–24. doi: 10.1016/8756-3282(86)90250-4
 144. Parisien M, Charhon S, Arlot M, Mainetti E, Chavassieux P, Chapuy MC, et al. Evidence for a Toxic Effect of Aluminium on Osteoblasts: A Histomorphometric Study in Hemodialysis Patients With Aplastic Bone Disease. *J Bone Miner Res* (1988) 3:259–67. doi: 10.1002/jbmr.5650030304
 145. Ott SM, Maloney NM, Klein GL. Aluminum is Associated With Low Bone Formation in Patients Receiving Chronic Parenteral Nutrition. *Ann Int Med* (1983) 98:910–14. doi: 10.7326/0003-4819-98-6-910
 146. Dalle Carbonare L, Mottes M, Valenti MT. Medication-Related Osteonecrosis of the Jaw (MRONJ): Are Antiresorptive Drugs the Main Culprits or Only Accomplices? The Triggering Role of Vitamin D Deficiency. *Nutrients* (2021) 13:561. doi: 10.3390/nu13020561
 147. Bedogni A, Saia G, Bettini G, Tronchet A, Totola A, Bedogni G, et al. Osteomalacia: The Missing Link in the Pathogenesis of Bisphosphonate-Related Osteonecrosis of the Jaws? *Oncologist* (2012) 17:1114–9. doi: 10.1634/theoncologist.2012-0141
 148. Sherrard DJ, Baylink DJ, Wergedal JE, Maloney NA. Quantitative Histological Studies on the Pathogenesis of Uremic Bone Disease. *J Clin Endocrinol Metab* (1974) 39:119–35. doi: 10.1210/jcem-39-1-119
 149. Malluche HH, Ritz E, Lange HP, Kutschera J, Hodgson M, Seiffert U, et al. Bone Histology in Incipient and Advanced Renal Failure. *Kidney Int* (1976) 9:355–62. doi: 10.1038/ki.1976.42
 150. KDIGO 2017 CLinical Practice Guideline Update for the Diagnosis, Evaluation, Prevention, and Treatment of Chronic Kidney Disease-Mineral and Bone Disorder (CKD-MBD). *Kidney Int Suppl* (2017) 7:1–59. doi: 10.1016/j.kisu.2017.04.001
 151. Dalle Carbonare L, Valenti MT, Giannini S, Gallieni M, Stefani F, Ciresa R, et al. Bone Biopsy for Histomorphometry in Chronic Kidney Disease (CKD): State-of-the-Art and New Perspectives. *J Clin Med* (2021) 10:4617. doi: 10.3390/jcm10194617
 152. Moe S, Druke T, Cunningham J, Goodman W, Martin K, Olgaard K, et al. Definition, Evaluation, and Classification of Renal Osteodystrophy: A Position Statement From Kidney Disease: Improving Global Outcomes (KDIGO). *Kidney Int* (2006) 69:1945–53. doi: 10.1038/sj.ki.5000414
 153. Malluche HH, Langub MC, Monier-Faugere MC. The Role of Bone Biopsy in Clinical Practice and Research. *Kidney Int* (1999) 73:S20–5. doi: 10.1046/j.1523-1755.1999.07313.x
 154. Malluche HH, Mawad HW, Monier-Faugere MC. Renal Osteodystrophy in the First Decade of the New Millennium: Analysis of 630 Bone Biopsies in Black and White Patients. *J Bone Miner Res* (2011) 26:1368–73. doi: 10.1002/jbmr.309
 155. Bouvard B, Pascaretti-Grizon F, Legrand E, Lavigne C, Audran M, Chappard D. Bone Lesions in Systemic Mastocytosis: Bone Histomorphometry and Histopathological. *Morphologie* (2020) 104:97–108. doi: 10.1016/j.morpho.2020.01.004
 156. Seitz S, Barvencik F, Koehne T, Priemel M, Pogoda P, Semler J, et al. Increased Osteoblast and Osteoclast Indices in Individuals With Systemic Mastocytosis. *Osteoporos Int* (2013) 24:2325–34. doi: 10.1007/s00198-013-2305-x
 157. Chavassieux P, Seeman E, Delmas PD. Insights Into Material and Structural Basis of Bone Fragility From Diseases Associated With Fractures: How Determinants of the Biomechanical Properties of Bone are Compromised by Disease. *Endocrine Rev* (2007) 28:151–64. doi: 10.1210/er.2006-0029
 158. Dalle Carbonare L, Micheletti V, Cosaro E, Valenti MT, Mottes M, Francia G, et al. Bone Histomorphometry in Acromegaly Patients With Fragility Vertebral Fractures. *Pituitary* (2018) 21:56–64. doi: 10.1007/s11102-017-0847-1
 159. Meunier PJ, Sellami S, Briançon D, Edouard C. Histological Heterogeneity of Apparently Idiopathic Osteoporosis. In: H Deluca, editor. *Osteoporosis. Recent Advances in Pathogenesis and Treatment*. Baltimore, USA: University Park Press (1981). p. 293–301.
 160. Teitelbaum SL, Bergfeld MA, Avioli LV, Whyte MP. Failure of Routine Biochemical Studies to Predict the Histological Heterogeneity of Untreated Postmenopausal Osteoporosis. In: H Deluca, editor. *Osteoporosis. Recent Advances in Pathogenesis and Treatment*. Baltimore, USA: University Park Press (1981). p. 303–9.
 161. Meunier PJ, Bressot C. Endocrine Influence on Bone Cells and Bone Remodeling Evaluated by Clinical Histomorphometry. In: JA Parsons, editor. *Endocrinology of Calcium Metabolism*. New York, USA: Raven Press (1982). p. 445–65.
 162. Parfitt AM. The Coupling of Bone Formation to Bone Resorption: A Critical Analysis of the Concept and of its Relevance to the Pathogenesis of Osteoporosis. *Metab Bone Dis Relat Res* (1982) 4:1–6. doi: 10.1016/0221-8747(82)90002-9
 163. Brown JP, Delmas PD, Malaval L, Edouard C, Chapuy MC, Meunier PJ. Serum Bone Gla-Protein: A Specific Marker for Bone Formation in Postmenopausal Osteoporosis. *Lancet* (1984) 1:1091–3. doi: 10.1016/s0140-6736(84)92506-6
 164. Eriksen EF, Hodgson SF, Eastell R, Cedel SL, O'Fallon WM, Riggs BL. Cancellous Bone Remodeling in Type I (Postmenopausal) Osteoporosis:

- Quantitative Assessment of Rates of Formation, Resorption, and Bone Loss at Tissue and Cellular Levels. *J Bone Miner Res* (1990) 5:311–9. doi: 10.1002/jbmr.5650050402
165. Arlot ME, Delmas PD, Chappard D, Meunier PJ. Trabecular and Endocortical Bone Remodeling in Postmenopausal Osteoporosis: Comparison With Normal Postmenopausal Women. *Osteoporos Int* (1990) 1:41–9. doi: 10.1007/BF01880415
 166. Van der Linden JC, Homminga J, Verhaar JAN, Weinans H. Mechanical Consequences of Bone Loss in Cancellous Bone. *J Bone Miner Res* (2001) 16:457–65. doi: 10.1359/jbmr.2001.16.3.457
 167. Viguet-Carrin S, Follet H, Gineys E, Roux JP, Munoz F, Chapurlat R, et al. Association Between Collagen Cross-Links and Trabecular Microarchitecture Properties of Human Vertebral Bone. *Bone* (2010) 46:342–7. doi: 10.1016/j.bone.2009.10.001
 168. Viguet-Carrin S, Roux JP, Arlot ME, Merabet Z, Leeming DJ, Byrjalsen I, et al. Contribution of the Advanced Glycation End Product Pentosidine and of Maturation of Type I Collagen to Compressive Biomechanical Properties of Human Lumbar Vertebrae. *Bone* (2006) 39:1073–9. doi: 10.1016/j.bone.2006.05.013
 169. Vashishth D, Gibson GJ, Khoury JI, Schaffler MB, Kimura J, Fyhr DP. Influence of Nonenzymatic Glycation on Biomechanical Properties of Cortical Bone. *Bone* (2001) 28:195–201. doi: 10.1016/s8756-3282(00)00434-8
 170. Tang SY, Zeenath U, Vashishth D. Effects of non-Enzymatic Glycation on Cancellous Bone Fragility. *Bone* (2007) 40:1144–51. doi: 10.1016/j.bone.2006.12.056
 171. Farlay D, Bala Y, Rizzo S, Bare S, Lappe JM, Recker R, et al. Bone Remodeling and Bone Matrix Quality Before and After Menopause in Healthy Women. *Bone* (2019) 128:115030. doi: 10.1016/j.bone.2019.08.003
 172. Hoffer CE, Guo XE, Zysset PK, Goldstein SA. An Application of Nanoindentation Technique to Measure Bone Tissue Lamellae Properties. *Biomech Eng* (2005) 127:1046–53. doi: 10.1115/1.2073671
 173. Hauge EM, Qvesel D, Eriksen EF, Mosekilde L, Melsen F. Cancellous Bone Remodeling Occurs in Specialized Compartments Lined by Cells Expressing Osteoblastic Markers. *J Bone Miner Res* (2001) 16:1575–82. doi: 10.1359/jbmr.2001.16.9.1575
 174. Parfitt AM. The Mechanism of Coupling: A Role for the Vasculature. *Bone* (2000) 26:319–23. doi: 10.1016/S8756-3282(00)80937-0
 175. Langdhal BL, Ralston SH. How Basic Science Discoveries Have Shaped the Treatment of Bone and Mineral Disorders. *J Bone Miner Res* (2017) 32:2324–30. doi: 10.1002/jbmr.3316
 176. Erben RG, Glösmann M. Histomorphometry in Rodents. *Methods Mol Biol* (2019) 1914:411–35. doi: 10.1007/978-1-4939-8997-3_24
 177. Boivin G, Chavassieux P, Chapuy MC, Baud CA, Meunier PJ. Skeletal Fluorosis: Histomorphometric Analysis of Bone Changes and Bone Fluoride Content in 29 Patients. *Bone* (1989) 10:89–99. doi: 10.1016/8756-3282(89)90004-5
 178. Briançon D, Meunier PJ. Treatment of Osteoporosis With Fluoride, Calcium and Vitamin D. *Orthop Clin North Am* (1981) 12:629–48. doi: 10.1016/S0030-5898(20)31375-4
 179. Lane JM, Healey JH, Schwartz E, Vigorita VJ, Schneider R, Einhorn TA, et al. Treatment of Osteoporosis With Sodium Fluoride and Calcium: Effects on Vertebral Fracture Incidence and Bone Histomorphometry. *Orthop Clin North Am* (1984) 15:729–45. doi: 10.1016/S0030-5898(20)31266-9
 180. Eriksen EF, Mosekilde L, Melsen F. Effect of Sodium Fluoride, Calcium, Phosphate, and Vitamin D on Trabecular Bone Balance and Remodeling in Osteoporotics. *Bone* (1985) 6:381–9. doi: 10.1016/8756-3282(85)90337-0
 181. Søgaard CH, Mosekilde L, Richards A, Mosekilde L. Marked Decrease in Trabecular Bone Quality After Five Years of Sodium Fluoride Therapy - Assessed by Biomechanical Testing of Iliac Crest Bone Biopsies in Osteoporotic Patients. *Bone* (1994) 15:393–9. doi: 10.1016/8756-3282(94)90815-x
 182. Fratz P, Roschger P, Eschberger J, Abendroth B, Klaushofer K. Abnormal Bone Mineralization After Fluoride Treatment in Osteoporosis: A Small-Angle X-Ray-Scattering Study. *J Bone Miner Res* (1994) 9:1541–9. doi: 10.1002/jbmr.5650091006
 183. Russell RGG, Watts NB, Ebtino FH, Rogers MJ. Mechanisms of Action of Bisphosphonates: Similarities and Differences and Their Potential Influence on Clinical Efficacy. *Osteoporos Int* (2008) 19:733–59. doi: 10.1007/s00198-007-0540-8
 184. Fleisch H. Bisphosphonates - History and Experimental Basis. *Bone* (1987) 8 Suppl 1:S23–8.
 185. Eriksen EF, Melsen F, Sod E, Barton I, Chines A. Effects of Long-Term Risedronate on Bone Quality and Bone Turnover in Women With Postmenopausal Osteoporosis. *Bone* (2002) 31:620–5. doi: 10.1016/s8756-3282(02)00869-4
 186. Recker RR, Ste-Marie L-G, Chavassieux P, McClung MR, Lundy MW. Bone Safety With Risedronate: Histomorphometric Studies at Different Dose Levels and Exposure. *Osteoporos Int* (2015) 26:327–37. doi: 10.1007/s00198-014-2850-y
 187. Recker RR, Weinstein RS, Chesnut CHIII, Schimmer RC, Mahoney P, Hughes C, et al. Histomorphometric Evaluation of Daily and Intermittent Oral Ibandronate in Women With Postmenopausal Osteoporosis: Results From the BONE Study. *Osteoporos Int* (2004) 15:231–7. doi: 10.1007/s00198-003-1530-0
 188. Recker RR, Delmas PD, Halse J, Reid IR, Boonen S, García-Hernandez PA, et al. Effects of Intravenous Zoledronic Acid Once Yearly on Bone Remodeling and Bone Structure. *J Bone Miner Res* (2008) 23:6–16. doi: 10.1359/jbmr.070906
 189. Bravenboer N, Papapoulos SE, Holzmann P, Hamdy NAT, Netelenbos JC, Lips P. Bone Histomorphometric Evaluation of Pamidronate Treatment in Clinically Manifest Osteoporosis. *Osteoporos Int* (1999) 9:489–93. doi: 10.1007/s001980050175
 190. Boivin G, Meunier PJ. Changes in Bone Remodeling Rate Influence the Degree of Mineralization of Bone. *Connect Tissue Res* (2002) 43:535–7. doi: 10.1080/03008200290000934
 191. Boivin GY, Chavassieux PM, Santora AC, Yates J, Meunier PJ. Alendronate Increases Bone Strength by Increasing the Mean Degree of Mineralization of Bone Tissue in Osteoporotic Women. *Bone* (2000) 27:687–94. doi: 10.1016/s8756-3282(00)00376-8
 192. Odvina CV, Zerwekh JE, Rao SD, Maalouf N, Gottschalk FA, Pak CYC. Severely Suppressed Bone Turnover: A Potential Complication of Alendronate Therapy. *J Clin Endocrinol Metab* (2005) 90:1294–301. doi: 10.1210/jc.2004-0952
 193. Mashiba T, Turner CH, Hirano T, Forwood M, Johnston CC, Burr DB. Effects of Suppressed Bone Turnover by Bisphosphonates on Microdamage Accumulation and Biochemical Properties in Clinically Relevant Skeletal Sites in Beagles. *Bone* (2001) 28:524–31. doi: 10.1016/s8756-3282(01)00414-8
 194. Chapurlat RD, Arlot M, Burt-Pichat B, Chavassieux P, Roux JP, Portero-Muzy N, et al. Microcrack Frequency and Bone Remodelling in Postmenopausal Osteoporotic Women on Long-Term Bisphosphonates: A Bone Biopsy Study. *J Bone Miner Res* (2007) 22:1502–9. doi: 10.1359/jbmr.070609
 195. Ott SM, Oleksik A, Yili L, Harper K, Lips P. Bone Histomorphometric and Biochemical Marker Results of a 2-Year Placebo-Controlled Trial of Raloxifene in Postmenopausal Women. *J Bone Miner Res* (2002) 17:341–8. doi: 10.1359/jbmr.2002.17.2.341
 196. Canalis E, Hott M, Deloffre P, Tsouderos Y, Marie PJ. The Divalent Strontium Salt S12911 Enhances Bone Cell Replication and Bone Formation *In Vitro*. *Bone* (1996) 18:517–23. doi: 10.1016/8756-3282(96)00080-4
 197. Takahashi N, Sasaki T, Tsouderos Y, Suda T. S1911-2 Inhibits Osteoclastic Bone Resorption *In Vitro*. *J Bone Miner Res* (2003) 18:1082–7. doi: 10.1359/jbmr.2003.18.6.1082
 198. Marie PJ, Hott M, Modrowski D, De Pollak C, Guillemain J, Deloffre P, et al. An Uncoupling Agent Containing Strontium Prevents Bone Loss by Depressing Bone Resorption and Maintaining Bone Formation in Estrogen-Deficient Rats. *J Bone Miner Res* (1993) 8:607–15. doi: 10.1002/jbmr.5650080512
 199. Arlot ME, Jiang Y, Genant HK, Zhao J, Burt-Pichat B, Roux JP, et al. Histomorphometric and μ CT Analysis of Bone Biopsies From Postmenopausal Osteoporotic Women Treated With Strontium Ranelate. *J Bone Miner Res* (2008) 23:215–22. doi: 10.1359/jbmr.071012
 200. Chavassieux P, Meunier PJ, Roux JP, Portero-Muzy N, Pierre M and Chapurlat R. Bone Histomorphometry of Transiliac Paired Bone Biopsies

- After 6 or 12 Months of Treatment With Oral Strontium Ranelate in 387 Osteoporotic Women: Randomized Comparison to Alendronate. *J Bone Miner Res* (2014) 29:618–28. doi: 10.1002/jbmr.2074
201. Falgayrac G, Farlay D, Ponçon C, Behal H, Gardegaront M, Ammann P, et al. Bone Matrix Quality in Paired Iliac Bone Biopsies From Postmenopausal Women Treated for 12 Months With Strontium Ranelate or Alendronate. *Bone* (2021) 153:116107. doi: 10.1016/j.bone.2021.116107
 202. Reeve J, Hesp R, Williams D, Klenerman L, Zanelli JM, Darby AJ, et al. Anabolic Effects of Low Dose of a Fragment of Human Parathyroid Hormone on the Skeleton in Postmenopausal Osteoporosis. *Lancet* (1976) 1:1035–8. doi: 10.1016/s0140-6736(76)92216-9
 203. Reeve J, Meunier PJ, Parsons JA, Bernat M, Bijvoet OLM, Courpron P, et al. Anabolic Effects of Human Parathyroid Hormone Fragment on Trabecular Bone in Involutional Osteoporosis: A Multicenter Trial. *Brit Med J* (1980) 280(6228):1340–4. doi: 10.1136/bmj.280.6228.1340
 204. Dempster DW, Cosman F, Kurland ES, Zhou H, Nieves J, Woelfert L, et al. Effect of Daily Treatment With Parathyroid Hormone on Bone Microarchitecture and Turnover in Patients With Osteoporosis: A Paired Biopsy Study. *J Bone Miner Res* (2001) 16:1846–53. doi: 10.1359/jbmr.2001.16.10.1846
 205. Arlot M, Meunier PJ, Boivin G, Haddock L, Tamayo J, Correa-Rotter R, et al. Differential Effects of Teriparatide and Alendronate on Bone Remodeling in Postmenopausal Women Assessed by Histomorphometric Parameters. *J Bone Miner Res* (2005) 20:1244–53. doi: 10.1359/JBMR.050309
 206. Hodsman AB, Kiesel M, Adachi JD, Fraher LJ, Watson PH. Histomorphometric Evidence for Increased Bone Turnover Without Change in Cortical Thickness or Porosity After 2 Years of Cyclical hPTH (1–34) Therapy in Women With Severe Osteoporosis. *Bone* (2000) 27:311–8. doi: 10.1016/s8756-3282(00)00316-1
 207. Hodsman AB, Steer BM. Early Histomorphometric Changes in Response to Parathyroid Hormone Therapy in Osteoporosis: Evidence for Novo Bone Formation on Quiescent Cancellous Surfaces. *Bone* (1993) 14:523–7. doi: 10.1016/8756-3282(93)90190-1
 208. Compston JE. Skeletal Actions of Intermittent Parathyroid Hormone: Effects on Bone Remodelling and Structure. *Bone* (2007) 40:1447–52. doi: 10.1016/j.bone.2006.09.008
 209. Moreira CA, Fitzpatrick LA, Wang Y, Recker RR. Effects of Abaloparatide-SC (BA058) on Bone Histology and Histomorphometry: The ACTIVE Phase 3 Trial. *Bone* (2017) 97:314–19. doi: 10.1016/j.bone.2016.11.004
 210. Miller PD, Hattersley G, Riis BJ, Williams GC, Lau E, Russo LA, et al. Effect of Abaloparatide vs Placebo on New Vertebral Fractures in Postmenopausal Women With Osteoporosis: A Randomized Clinical Trial. *JAMA* (2016) 316:722–33. doi: 10.1001/jama.2016.11136
 211. Chavassieux P, Karsdal MA, Segovia-Silvestre T, Neutsky-Wulf AV, Chapurlat R, Boivin G, et al. Mechanisms of the Anabolic Effects of Teriparatide on Bone: Insight From the Treatment of a Patient With Pycnodysostosis. *J Bone Miner Res* (2008) 23:1076–83. doi: 10.1359/jbmr.080231
 212. Fratzl-Zelman N, Valenta A, Roschger P, Nader A, Gelb BD, Fratzl P, et al. Decreased Bone Turnover and Deterioration of Bone Structure in Two Cases of Pycnodysostosis. *J Clin Endocrinol Metab* (2004) 89:1538–47. doi: 10.1210/jc.2003-031055
 213. Drake MT, Clarke BL, Oursler MJ, Khosla S. Cathepsin K Inhibitors for Osteoporosis: Biology, Potential Clinical Utility, and Lessons Learned. *Endocrine Rev* (2017) 38:325–50. doi: 10.1210/er.2015-1114
 214. Bone HG, McClung MR, Roux C, Recker RR, Eisman JA, Verbruggen N, et al. Odanacatib, a Cathepsin-K Inhibitor for Osteoporosis: A Two-Year Study in Postmenopausal Women With Low Bone Density. *J Bone Miner Res* (2010) 25:937–47. doi: 10.1359/jbmr.091035
 215. Recker R, Dempster D, Langdahl B, Giezek H, Clark S, Ellis G, et al. Effects of Odanacatib on Bone Structure and Quality in Postmenopausal Women With Osteoporosis: 5-Year Data From the Phase 3 Long-Term Odanacatib Fracture Trial (LOFT) and its Extension. *J Bone Miner Res* (2020) 35:1289–99. doi: 10.1002/jbmr.3994
 216. Reid IR, Miller PD, Brown JP, Kendler DL, Fahrleitner-Pammer A, Valter I, et al. Effects of Denosumab on Bone Histomorphometry: The FREEDOM and STAND Studies. *J Bone Miner Res* (2010) 25:2256–65. doi: 10.1002/jbmr.149
 217. Brown JP, Reid IR, Wagman RB, Kendler D, Miller PD, Beck Jensen JE, et al. Effects of Up to 5 Years of Denosumab Treatment on Bone Histology and Histomorphometry: The FREEDOM Study Extension. *J Bone Miner Res* (2014) 29:2051–56. doi: 10.1002/jbmr.2236
 218. Dempster DW, Brown JP, Fahrleitner-Pammer A, Kendler D, Rizzo S, Valter I, et al. Effects of Long-Term Denosumab on Bone Histomorphometry and Mineralization in Women With Postmenopausal Osteoporosis. *J Clin Endocrinol Metab* (2018) 103:2498–509. doi: 10.1210/jc.2017-02669
 219. Brown JP, Dempster DW, Ding B, Dent-Acosta R, San Martin J, Grauer A, et al. Bone Remodeling in Postmenopausal Women Who Discontinued Denosumab Treatment: Off-Treatment Biopsy Study. *J Bone Miner Res* (2011) 26:2737–44. doi: 10.1002/jbmr.448
 220. Chavassieux P, Portero-Muzy N, Roux JP, Horlait S, Dempster DW, Wang A, et al. Reduction of Cortical Bone Turnover and Erosion Depth After 2 and 3 Years of Denosumab: Iliac Bone Histomorphometry in the FREEDOM Trial. *J Bone Miner Res* (2019) 34:626–31. doi: 10.1002/jbmr.3631
 221. Dempster DW, Zhou H, Recker RR, Brown JP, Recknor CP, Lewiecki EM, et al. Remodeling- and Modeling-Based Bone Formation With Teriparatide Versus Denosumab: A Longitudinal Analysis From Baseline to 3 Months in the AVA Study. *J Bone Miner Res* (2018) 33:298–306. doi: 10.1002/jbmr.3309
 222. Ubara Y, Tagami T, Nakanishi S, Sawa N, Hoshino J, Suwabe T, et al. Significance of Minimization in Dialysis Patients With Adynamic Bone Disease. *Kidney Int* (2005) 68:833–9. doi: 10.1111/j.1523-1755.2005.00464.x
 223. Zebaze R, Libanati C, McClung MR, Zanchetta JR, Kendler DL, Hoiseth A, et al. Denosumab Reduces Cortical Porosity of the Proximal Femoral Shaft in Postmenopausal Women With Osteoporosis. *J Bone Miner Res* (2016) 31:1827–34. doi: 10.1002/jbmr.2855
 224. Makras P, Polyzos SA, Papatheodorou A, Kokkoris P, Chatzifotiadis D, Anastasilakis AD. Parathyroid Hormone Changes Following Denosumab Treatment in Postmenopausal Osteoporosis. *Clin Endocrinol (Oxf)* (2013) 79:499–503. doi: 10.1111/cen.12188
 225. Dempster DW, Zhou H, Recker RR, Brown JP, Recknor CP, Lewiecki EM, et al. Differential Effects of Teriparatide and Denosumab on Intact PTH and Bone Formation Indices: AVA Osteoporosis Study. *J Clin Endocrinol Metab* (2016) 101:1353–63. doi: 10.1210/jc.2015-4181
 226. Van Lierop AH, Appelman-Dijkstra N, Papapoulos SE. Sclerostin Deficiency in Humans. *Bone* (2017) 96:51–62. doi: 10.1016/j.bone.2016.10.010
 227. Ominsky MS, Niu QT, Li C, Li X, Ke HZ. Tissue-Level Mechanisms Responsible for the Increase in Bone Formation and Bone Volume by Sclerostin Antibody. *J Bone Miner Res* (2014) 29:1424–30. doi: 10.1002/jbmr.2152
 228. Boyce RW, Niu QT, Ominsky MS. Kinetic Reconstruction Reveals Time-Dependent Effects of Romosozumab on Bone Formation and Osteoblast Function in Vertebral Cancellous and Cortical Bone in Cynomolgus Monkeys. *Bone* (2017) 101:77–87. doi: 10.1016/j.bone.2017.04.005
 229. Eriksen EF, Chapurlat R, Boyce RW, Shi Y, Brown JP, Horlait S, et al. Modeling-Based Bone Formation After 2 Months of Romosozumab Treatment: Results From the FRAME Clinical Trial. *J Bone Miner Res* (2022) 37:36–40. doi: 10.1002/jbmr.4457
 230. Boyce RW, Brown D, Felix M, Mellal N, Locher K, Pyrah I, et al. Decreased Osteoprogenitor Proliferation Precedes Attenuation of Cancellous Bone Formation in Ovariectomized Rats Treated With Sclerostin Antibody. *Bone Rep* (2018) 8:90–4. doi: 10.1016/j.bonr.2018.03.001
 231. LeCun Y, Bengio Y, Hinton G. Deep Learning. *Nature* (2015) 521:436–44. doi: 10.1038/nature14539
 232. Xing F, Xie Y, Su H, Liu F, Yang L. Deep Learning in Microscopy Image Analysis: A Survey. *IEEE Trans Neural Netw Learn Syst* (2018) 29:4550–68. doi: 10.1109/TNNLS.2017.2766168
 233. Song T-H, Sanchez V, ElDaly H, Rajpoot NM. Simultaneous Cell Detection and Classification in Bone Marrow Histology Images. *IEEE J BioMed Health Inform* (2019) 23:1469–76. doi: 10.1109/JBHI.2018.2878945
 234. Smets J, Shevroja E, Hügle T, Leslie WD, Hans D. Machine Learning Solutions for Osteoporosis—A Review. *J Bone Miner Res* (2021) 36:833–51. doi: 10.1002/jbmr.4292
 235. Baron R. Importance of the Intermediate Phases Between Resorption and Formation in the Measurement and Understanding of the Bone Remodeling Sequence. In: PJ Meunier, editor. *Bone Histomorphometry: Second*

- International Workshop*. Toulouse: Société Nouvelle Imprimerie Fournié (1976). p. 179–83.
236. Eriksen EF, Gundersen HJ, Melsen F, Mosekilde L. Reconstruction of the Formative Site in Iliac Trabecular Bone in 20 Normal Individuals Employing a Kinetic Model for Matrix and Mineral Apposition. *Metab Bone Dis Relat Res* (1984) 5:243–52. doi: 10.1016/0221-8747(84)90066-3
 237. Andersen TL, Abdelgawad ME, Kristensen HB, Hauge EM, Rolighed L, Bollerslev J, et al. Understanding Coupling Between Bone Resorption and Formation: Are Reversal Cells the Missing Link? *Am J Pathol* (2013) 183:235–46. doi: 10.1016/j.ajpath.2013.03.006
 238. Sims NA, Civitelli R. Cell-Cell Signaling: Broadening Our View of the Basic Multicellular Unit. *Calcif Tissue Int* (2014) 94:2–3. doi: 10.1007/s00223-013-9766-y
 239. Teti A. Mechanisms of Osteoclast-Dependent Bone Formation. *Bonekey Rep* (2013) 2:449. doi: 10.1038/bonekey.2013.183
 240. Andersen TL, Sondergaard TE, Skorzynska KE, Dagnaes-Hansen F, Plesner TL, Hauge EM, et al. A Physical Mechanism for Coupling Bone Resorption and Formation in Adult Human Bone. *Am J Pathol* (2009) 174:239–47. doi: 10.2353/ajpath.2009.080627
 241. Andersen TL, Hauge EM, Rolighed L, Bollerslev J, Kjaersgaard-Andersen P, Delaisse JM. Correlation Between Absence of Bone Remodeling Compartment Canopies, Reversal Phase Arrest, and Deficient Bone Formation in Post-Menopausal Osteoporosis. *Am J Pathol* (2014) 184:1142–51. doi: 10.1016/j.ajpath.2013.12.005
 242. Andersen TL, Soe K, Sondergaard TE, Plesner T, Delaisse JM. Myeloma Cell-Induced Disruption of Bone Remodelling Compartments Leads to Osteolytic Lesions and Generation of Osteoclast-Myeloma Hybrid Cells. *Br J Haematol* (2010) 148:551–61. doi: 10.1111/j.1365-2141.2009.07980.x
 243. Jensen PR, Andersen TL, Soe K, Hauge EM, Bollerslev J, Amling M, et al. Premature Loss of Bone Remodeling Compartment Canopies is Associated With Deficient Bone Formation: A Study of Healthy Individuals and Patients With Cushing's Syndrome. *J Bone Miner Res* (2012) 27:770–80. doi: 10.1002/jbmr.1490
 244. Jensen PR, Andersen TL, Hauge EM, Bollerslev J, Delaisse JM. A Joined Role of Canopy and Reversal Cells in Bone Remodeling - Lessons From Glucocorticoid-Induced Osteoporosis. *Bone* (2015) 73:16–23. doi: 10.1016/j.bone.2014.12.004
 245. Abdelgawad ME, Delaisse JM, Hinge M, Jensen PR, Alnaimi RW, Rolighed L, et al. Early Reversal Cells in Adult Human Bone Remodeling: Osteoblastic Nature, Catabolic Functions and Interactions With Osteoclasts. *Histochem Cell Biol* (2016) 145:603–15. doi: 10.1007/s00418-016-1414-y
 246. Everts V, Delaisse JM, Korper W, Jansen DC, Tigchelaar-Gutter W, Saftig P, et al. The Bone Lining Cell: Its Role in Cleaning Howship's Lacunae and Initiating Bone Formation. *J Bone Miner Res* (2002) 17:77–90. doi: 10.1359/jbmr.2002.17.1.77
 247. Lassen NE, Andersen TL, Ploen GG, Soe K, Hauge EM, Harving S, et al. Coupling of Bone Resorption and Formation in Real Time: New Knowledge Gained From Human Haversian BMUs. *J Bone Miner Res* (2017) 32:1395–405. doi: 10.1002/jbmr.3091
 248. Kristensen HB, Andersen TL, Marcussen N, Rolighed L, Delaisse JM. Increased Prevalence of Capillaries Next to Remodeling Sites in Adults Human Cancellous Bone. *J Bone Miner Res* (2013) 28:574–85. doi: 10.1002/jbmr.1760
 249. Jensen PR, Andersen TL, Chavassieux P, Roux JP, Delaisse JM. Bisphosphonates Impair the Onset of Bone Formation at Remodeling Sites. *Bone* (2021) 145:115850. doi: 10.1016/j.bone.2021.115850
 250. Hattner R, Epker BN, Frost HM. Suggested Sequential Mode of Control of Changes in Cell Behaviour in Adult Bone Remodelling. *Nature* (1965) 206(983):489–90. doi: 10.1038/206489a0
 251. Langdahl B, Ferrari S, Dempster DW. Bone Modeling and Remodeling: Potential as Therapeutic Targets for the Treatment of Osteoporosis. *Ther Adv Musculoskel Dis* (2016) 8:225–35. doi: 10.1177/1759720X16670154
 252. McDonald MC, Khoo WH, Ng PY, Xiao Y, Zamerli J, Thatcher P, et al. Osteoclasts Recycle via Osteomorphs During RANKL-Stimulated Bone Resorption. *Cell* (2021) 184:1330–47. doi: 10.1016/j.cell.2021.02.002
- Conflict of Interest:** The authors declare that the research was conducted in the absence of any commercial or financial relationships that could be construed as a potential conflict of interest.
- Publisher's Note:** All claims expressed in this article are solely those of the authors and do not necessarily represent those of their affiliated organizations, or those of the publisher, the editors and the reviewers. Any product that may be evaluated in this article, or claim that may be made by its manufacturer, is not guaranteed or endorsed by the publisher.
- Copyright © 2022 Chavassieux and Chapurlat. This is an open-access article distributed under the terms of the Creative Commons Attribution License (CC BY). The use, distribution or reproduction in other forums is permitted, provided the original author(s) and the copyright owner(s) are credited and that the original publication in this journal is cited, in accordance with accepted academic practice. No use, distribution or reproduction is permitted which does not comply with these terms.